TEZ ŞABLONU ONAY FORMU
THESIS TEMPLATE CONFIRMATION FORM

1. Şablonda verilen yerleşim ve boşluklar değiştirilmemelidir.
2. **Jüri tarihi** Başlık Sayfası, İmza Sayfası, Abstract ve Öz'de ilgili yerlere yazılmalıdır.
3. İmza sayfasında jüri üyelerinin unvanları doğru olarak yazılmalıdır. Tüm imzalar **mavi pilot kalemle** atılmalıdır.
4. **Disiplinlerarası** programlarda görevlendirilen öğretim üyeleri için jüri üyeleri kısmında tam zamanlı olarak çalıştıkları anabilim dalı başkanlığının ismi yazılmalıdır. Örneğin: bir öğretim üyesi Biyoteknoloji programında görev yapıyor ve biyoloji bölümünde tam zamanlı çalışıyorsa, İmza sayfasına biyoloji bölümü yazılmalıdır. İstisnai olarak, disiplinler arası program başkanı ve tez danışmanı için disiplinlerarası program adı yazılmalıdır.
5. Tezin **son sayfasının sayfa** numarası Abstract ve Öz'de ilgili yerlere yazılmalıdır.
6. Bütün chapterlar, referanslar, ekler ve CV sağ sayfada başlamalıdır. Bunun için **kesmeler** kullanılmıştır. **Kesmelerin kayması** fazladan boş sayfaların oluşmasına sebep olabilir. Bu gibi durumlarda paragraf (¶) işaretine tıklayarak kesmeleri görünür hale getirin ve yerlerini **kontrol edin**.
7. Figürler ve tablolar kenar boşluklarına taşmamalıdır.
8. Şablonda yorum olarak eklenen uyarılar dikkatle okunmalı ve uygulanmalıdır.
9. Tez yazdırılmadan önce PDF olarak kaydedilmelidir. Şablonda yorum olarak eklenen uyarılar PDF dokümanında yer almamalıdır.
10. Tez taslaklarının kontrol işlemleri tamamlandığında, bu durum öğrencilere METU uzantılı öğrenci e-posta adresleri aracılığıyla duyurulacaktır.
11. Tez yazım süreci ile ilgili herhangi bir sıkıntı yaşarsanız, **Sıkça Sorulan Sorular (SSS)** sayfamızı ziyaret ederek yaşadığınız sıkıntıyla ilgili bir çözüm bulabilirsiniz.

1. Do not change the spacing and placement in the template.
2. Write **defense date** to the related places given on Title page, Approval page, Abstract and Öz.
3. Write the titles of the examining committee members correctly on Approval Page. **Blue ink** must be used for all signatures.
4. For faculty members working in **interdisciplinary programs**, the name of the department that they work full-time should be written on the Approval page. For example, if a faculty member staffs in the biotechnology program and works full-time in the biology department, the department of biology should be written on the approval page. Exceptionally, for the interdisciplinary program chair and your thesis supervisor, the interdisciplinary program name should be written.
5. Write **the page number of the last page** in the related places given on Abstract and Öz pages.
6. All chapters, references, appendices and CV must be started on the right page. **Section Breaks** were used for this. **Change in the placement** of section breaks can result in extra blank pages. In such cases, make the section breaks visible by clicking paragraph (¶) mark and **check their position.**
7. All figures and tables must be given inside the page. Nothing must appear in the margins.
8. All the warnings given on the comments section through the thesis template must be read and applied.
9. Save your thesis as pdf and Disable all the comments before taking the printout.
10. This will be announced to the students via their METU students e-mail addresses when the control of the thesis drafts has been completed.
11. If you have any problems with the thesis writing process, you may visit our **Frequently Asked Questions (FAQ)** page and find a solution to your problem.

☒ **Yukarıda bulunan tüm maddeleri okudum, anladım ve kabul ediyorum. / I have read, understand and accept all of the items above.**

Name :
Surname :
E-Mail :
Date :
Signature : _____

ANALYSIS OF MAGNETOHYDRODYNAMICS PROBLEMS USING OPENFOAM

A THESIS SUBMITTED TO
THE GRADUATE SCHOOL OF NATURAL AND APPLIED SCIENCES
OF
MIDDLE EAST TECHNICAL UNIVERSITY

BY

NERGİS GÜNDÜZ

IN PARTIAL FULFILLMENT OF THE REQUIREMENTS
FOR
THE DEGREE OF MASTER OF SCIENCE
IN
AEROSPACE ENGINEERING

DECEMBER 2023

Approval of the thesis:

ANALYSIS OF MAGNETOHYDRODYNAMICS PROBLEMS USING OPENFOAM

submitted by **NERGİS GÜNDÜZ** in partial fulfillment of the requirements for the degree of **Master of Science** i**n Aerospace Engineering, Middle East Technical University** by,

Prof. Dr. Halil Kalıpçılar
Dean, **Graduate School of Natural and Applied Sciences** _____

Prof. Dr. Serkan Özgen
Head of the Department, **Aerospace Engineering** _____

Prof. Dr. Sinan Eyi
Supervisor, **Aerospace Engineering Department, METU** _____

Examining Committee Members:

Prof. Dr. Dilek Funda Kurtuluş
Department of Aerospace Engineering, METU _____

Prof. Dr.Sinan Eyi
Department of Aerospace Engineering , METU _____

Prof. Dr.Nilay Sezer Uzol
Department of Aerospace Engineering, METU _____

Prof. Dr. Serhat Çakır
Department of Science and Technology, Başkent University _____

Assoc. Dr. Sıtkı Uslu
Department of Mechanical Engineering., TEDU _____

Date: 21.12.2023

I hereby declare that all information in this document has been obtained and presented in accordance with academic rules and ethical conduct. I also declare that, as required by these rules and conduct, I have fully cited and referenced all material and results that are not original to this work.

Name Last Name: Nergis Gündüz

Signature:

ABSTRACT

ANALYSIS OF MAGNETOHYDRODYNAMICS PROBLEMS USING OPENFOAM

Gündüz, Nergis
Master of Science, Aerospace Engineering
Supervisor: Prof. Dr. Sinan Eyi

December 2023, 81 pages

The thesis aims to simulate 3-D Orszag-Tang vortex and Shock-Cloud interaction test problem via an open source code OpenFOAM. The incompressible 3-D Orszag-Tang vortex and 2-D compressible shock-cloud interaction problems have been used as benchmark problems and standard test cases for codes. Also, there are other common test problems like rotor test-rig, shock tube, and 3-D blast problem. However, occurrance of MHD shocks besides vortex observation is possible.

The simulation belongs to Magnetohydrodynamics (MHD) area. In the problem plasmas and magnetic field lines run together. Especially movement of magnetic, electrically conducting fluids directly related with the direction of magnetic area. Both compressible, incompressible or pressure based, density-based versions exist, possible to observe in different Mach numbers MHD equations have become extensive tools for space plasmas. Combination of Maxwell and Navier-Stokes equations are implemented at solution of the problems. Pressure-Implicit with Splitting of Operators (PISO) algorithm is used in solvers by OpenFOAM which

include the conservation equations for mass, momentum, energy, and magnetic induction respectively.

Keywords: 3-D Orsag-Tang vortex, 2-D Shock-Cloud Interaction, MHD, mhdFoam

ÖZ

MAGNETOHİDRODİNAMİK PROBLEMLERİNİN OPENFOAM İLE ANALİZİ

Gündüz, Nergis
Yüksek Lisans, Havacılık ve Uzay Mühendisliği
Tez Yöneticisi: Prof. Dr. Sinan Eyi

Aralık 2023, 81 sayfa

Bu tez, 3-B Orszag-Tang girdabı ve şok-bulut etkileşimi test problemini açık kaynak kodlu OpenFOAM ile simüle etmeyi amaçlamaktadır. Sıkıştırılamaz 3-B Orszag-Tang Girdabı ve 2-B sıkıştırılabilir Şok-Bulut Etkileşimi problemlerinin oluşturulması, kodlar için bir karşılaştırma problemleri ve standart testler kullanılarak yapılmıştır. Ayrıca Rotor Test-Rig, Şok Tüpü ve 3-D Patlama problemi gibi diğer yaygın test problemleri de vardır. Ancak, bu problemin tercih edilmesi, girdap gözleminin yanı sıra MHD şoklarının oluşumunu ele alma şansı vermesine dayanmaktadır.

Simülasyon Magnetohidrodinamik (MHD) alanına aittir ve problemde plazmalar ve manyetik alan çizgileri birlikte çalışır. Özellikle manyetik, elektriksel olarak iletken, akışkanların hareketi doğrudan manyetik alanın yönü ile ilgilidir. Hem sıkıştırılabilir, hem sıkıştırılamaz veya basınç tabanlı, yoğunluk tabanlı versiyonları mevcuttur, farklı mach sayılarında gözlemlemek mümkündür MHD denklemleri uzay plazmaları için kapsamlı araçlar haline gelmiştir. OpenFOAM'ın çözücülerinde sırasıyla kütle, momentum, enerji ve manyetik indüksiyon için

korunum denklemlerini içeren Operatörlerin Bölünmesi ile Basınç Örtük (PISO) algoritması kullanılır.

Anahtar Kelimeler: 3 Boyutlu Orsag-Tang girdabı, 2 Boyutlu şok bulut etkileşimi, MHD, mhdFoam

To Ardan,

ACKNOWLEDGMENTS

I am grateful to my supervisor Prof. Dr. Sinan Eyi for his support, guidance and encouragement of me to succeed the process. He is a great mentor who really and deeply devotes himself to his students to teach. Moreover, I am thankful to him for sharing his valuable knowledge and experiences with me while I am studying on the thesis.

In addition to my advisor, I am also grateful to Prof. Dr. Serhat Çakır for his insightful comments, encouragement and reviewing of my work.

I would like to thank to assistants; Melikşah Koca, Can Erdoğan, Halime Gül Demirer, İldeniz Öztürk from the Department of Aerospace Engineering who have answered my questions when I need to complete misunderstanding points. Also, I would like to thank my friends working at Simulation, Control and Avionics Laboratory. Moreover, I would like to thank both my best friends Aysun Asena Aslan and Sercan Güngör.

Finally, I would like to express my gratitude to my large, beautiful family for all their pure love, support, and their encouragements while I am writing this thesis.

TABLE OF CONTENTS

LIST OF TABLES

TABLES

LIST OF FIGURES

FIGURES

LIST OF SYMBOLS

SYMBOLS

Symbol	Description	Units
g	Gravitational acceleration	m/s2
h	Convective heat transfer coefficient	W/m C
k	thermal of conductivity	W/m°C
L	length	m
W	width	m
H	thickness	m
x, y, z	Cartesian Coordinates	-
u, v, w	Velocities of fluids in x, y and z-directions respectively	m/s
t	Time	s
T	Temperature	°C
T∞	Surrounding temperature	°C
Tb	base temperature	°C
Greek Letters		
ρ	Density	kg/m^3
μ	Dynamic viscosity	Pa.s
α	Thermal diffusivity	m^2/s
σ	Shear stress	N/m^2
c	Specific heat ratio	J/k K
η	efficiency	-

CHAPTER 1

INTRODUCTION

Magnetohydrodynamics (MHD) is a branch of fluid mechanics that investigates the behaviors of electrically conducting fluids under magnetic fields. MHD is a multidisciplinary field that draws upon principles from fluid mechanics, electromagnetism, and plasma physics, and has numerous applications, ranging from astrophysics to energy generation and industrial processes [1-5]. In MHD schemes, the fluid is typically a conducting liquid metal or plasma. When a magnetic field is applied to the fluid, it induces an electric current that generates a corresponding magnetic field. The interaction between the magnetic fields and fluid motion leads to complex phenomena such as turbulence, instabilities, and electromagnetic waves. MHD is vital for studying magnetospheres, which are areas of space surrounding planets and stars where the magnetic field dominates the plasma behaviors. For instance, the Earth's magnetosphere is where the planet's magnetic field interacts with the solar wind, a stream of charged particles from the Sun.

1.1 Applications of MHD

MHD simulations help scientists understand plasma behaviors in the magnetosphere and develop models that predict space weather, which can affect satellite operations and power grids. MHD is also crucial in energy generation, particularly in the development of fusion reactors that aim to replicate the Sun's nuclear fusion reactions. The fuel in a fusion reactor is plasma of hydrogen isotopes confined by a magnetic field. MHD simulations optimize the magnetic field and plasma

confinement design to achieve sustainable fusion reactions. In industrial processes, MHD has applications such as stirring and mixing fluids, transporting heat, and generating electricity. For instance, liquid metals are used in nuclear reactor cooling, where MHD controls the metal flow and generates electricity through the interaction between the magnetic field and the moving fluid. In conclusion, Magnetohydrodynamics is an exciting branch of fluid mechanics those studies electrically conducting fluids' behaviors under magnetic fields. MHD has vast applications, including astrophysics, energy generation, and industrial processes. MHD simulations provide insights into complex phenomena in these schemes and help optimize their design and operation [5].

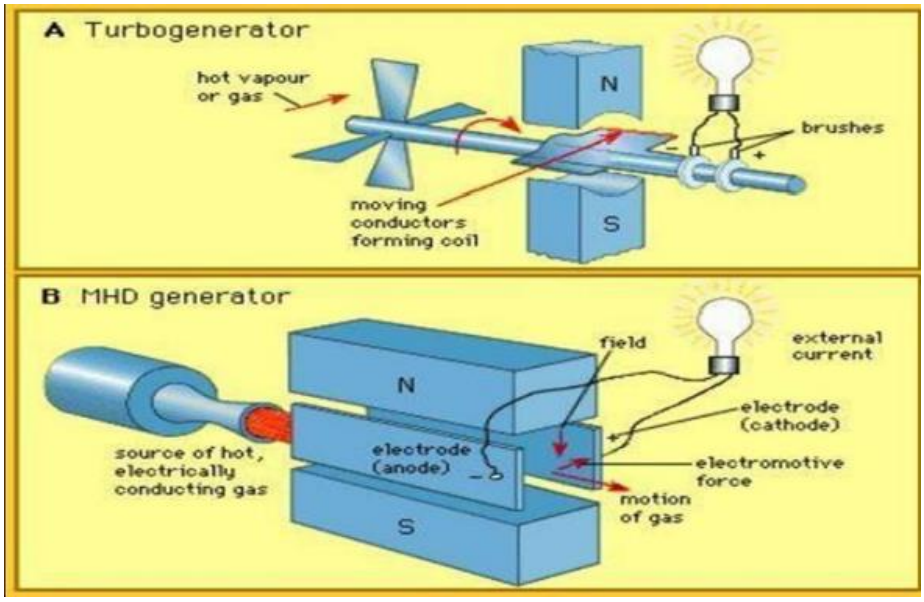

Figure 1.1 Applications of MHD in power generator [5]

A vortex refers to the swirling motion of fluid that occurs when fluid layers rotate or shear. Vortices are prevalent in numerous fluid schemes, such as the Earth's atmosphere and oceans, as well as in industrial processes, including mixing and stirring. When an electrically conducting fluid is exposed to a magnetic field, it

induces an electric current that leads to a magnetic field's generation. The interaction between the magnetic fields and fluid motion can result in complex phenomena, such as vortex generation. In Magnetohydrodynamics (MHD), a vortex can be created by flowing a conducting fluid in a magnetic field's presence. The interaction between

the magnetic field and fluid motion causes the fluid to twist, leading to vortex formation. The vortex's size, shape, and stability can be influenced by the magnetic field's strength and direction. The study of MHD vortices has various applications, such as designing industrial processes, including mixing and stirring, and understanding plasma behaviors in fusion reactors. For example, MHD vortices can be utilized in chemical reactions to mix fluids or cool nuclear reactors. In summary, MHD is an intriguing subfield of fluid mechanics those studies electrically conducting fluids under magnetic fields. Vortex generation is a complex phenomenon that can be produced by the interaction between magnetic fields and fluid motion. This phenomenon has broad applications in various fields, including industrial processes and fusion energy research [6-7].

The 3D Orszag-Tang vortex serves as a fundamental problem in fluid dynamics and is commonly employed to investigate vortex and turbulence dynamics. It is an expansion of the 2D Orszag-Tang vortex, which was established by Orszag and Tang in 1979 as a simplified model of the interaction between a vortex and a shock wave in a compressible fluid. The 3D Orszag-Tang vortex is created by the interaction of two counter-rotating vortices positioned initially at the center of a cubic domain that has a uniform fluid. With opposite spin directions, the vortices produce a shear layer between them, which becomes unstable because of the Kelvin-Helmholtz instability.

As the instabilities develop, the shear layer turns increasingly turbulent, and the vortices begin to interact, producing a complex flow pattern comprising smaller vortices, filaments, and eddies. Eventually, the flow achieves equilibrium, with the vortices merging and the flow becoming fully turbulent. The 3D Orszag-Tang vortex is a standard test problem to evaluate numerical methods and turbulence models because of the big range of spatial and temporal scales it exhibits.

Furthermore, it displays complex flow characteristics such as vortex stretching, folding, and reconnection, making it a useful test case for examining the impact of compressibility, viscosity, and magnetic fields on turbulence.

Overall, the 3D Orszag-Tang vortex is a valuable tool for comprehending turbulent flow dynamics and developing more precise and efficient numerical methods to simulate them [8]. The 3D Orszag-Tang vortex boasts an abundance of applications in the exploration of fluid flow dynamics. Its principal function is as a benchmark issue for testing and authenticating numerical techniques and turbulence models. The intricate flow features of the vortex, including the interplay between counter- rotating vortices and the genesis of instabilities, render it a superbtest case for assessing the precision and efficiency of computational fluid dynamics (CFD) simulations.

Moreover, the vortex is an invaluable instrument for scrutinizing the dynamics of turbulent flows. Turbulence, a universal phenomenon in fluid dynamics, is signified by the erratic movement of fluids. The 3D Orszag-Tang vortex provides a simplified archetype for scrutinizing the fundamental mechanisms of turbulence, such as vortex stretching and folding, thereby enabling researchers to refine their comprehension of intricate flow behaviors within real-world fluid schemes. The 3D Orszag-Tang vortex is also pertinent to the study of compressible fluid flow.

Compressible fluids alter their density significantly due to changes in pressure and temperature. The confluence of vortices in the 3D Orszag-Tang vortex engenders a shock wave, rendering it an expedient test case for investigating the effects of compressibility on fluid flow. Lastly, the vortex is utilized to examine the influence of magnetic fields on fluid flow. Magnetic fields can exert a substantial impact on fluid behaviors, particularly in the realm of plasma physics.

By incorporating a magnetic field into the 3D Orszag-Tang vortex simulation, researchers can scrutinize the interaction between magnetic fields and fluid flow, which has applications in diverse fields, including astrophysics and fusion energy research.

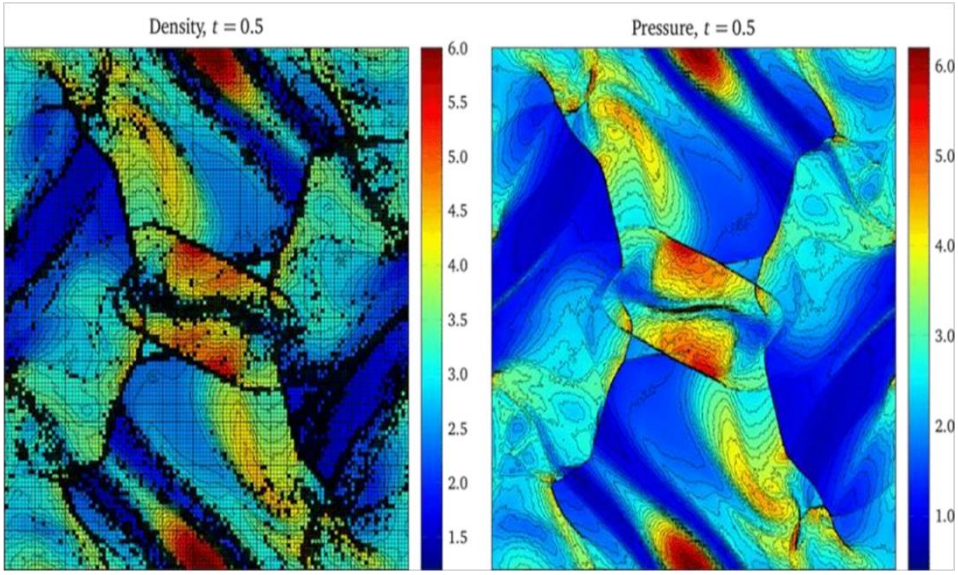

Figure 1.2. The 3-D Orszag-Tang vortex in literature [8]

In summary, the 3D Orszag-Tang vortex is a versatile tool with a plenitude of applications in a diverse range of fluid flow research areas, encompassing CFD simulations, turbulence studies, compressible fluid flow, and the effects of magnetic fields on fluid dynamics [8].

1.2 Various Vortex Flows in Fluid Dynamics

Vortices are common in fluid dynamics, and they play a critical role in many natural and engineering schemes. A vortex is a swirling motion of fluid particles that can be observed in a big range of scales, from the small-scale vortex shedding behind a cylinder to the large-scale vortices in the Earth's atmosphere. In this article, we will discuss various vortex types and their significance in fluid dynamics.

1.2.1 Rankine Vortex

The Rankine vortex is a simple model of a vortex that is often used as a benchmark problem for vortex simulations. It is a two-dimensional vortex that has a constant vorticity and a Gaussian radial velocity profile. The Rankine vortex is an idealized model of vortices that occur in real-life systems such as the wake behind a ship [9].

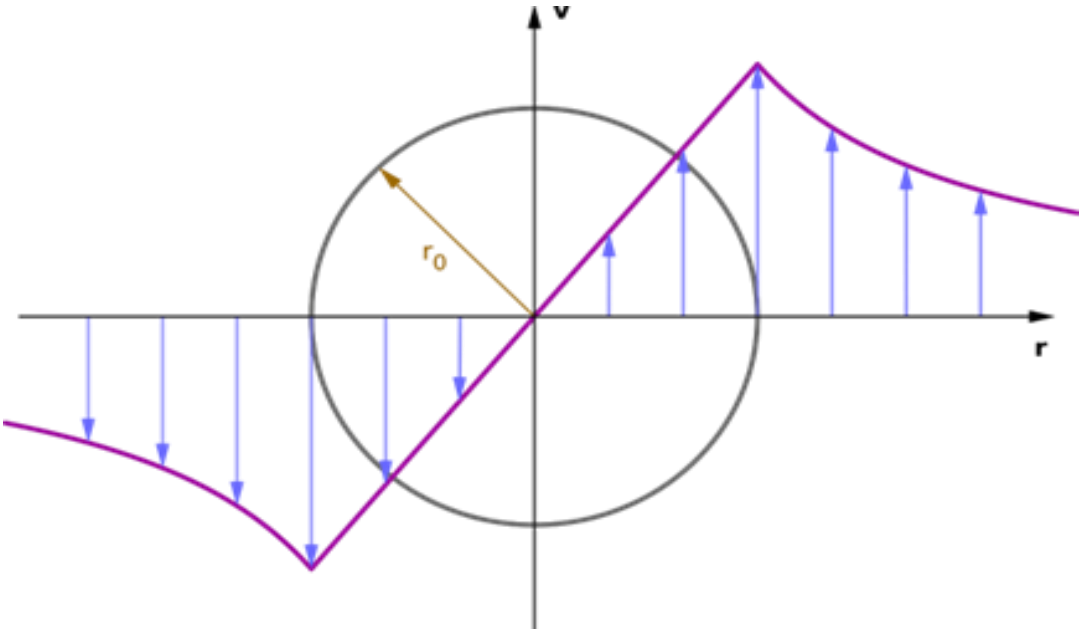

Figure 1.3. Rankine Vortex [9]

1.2.2 Lamb-Oseen vortex

The Lamb-Oseen vortex is a model of a vortex that has a radial velocity profile that decays exponentially with distance from the vortex center. The Lamb-Oseen vortex is a more realistic model of a vortex than the Rankine vortex and is often used in

vortex simulations. The Lamb-Oseen vortex is also used as a model of vortices that occur in real-life systems, such as the vortex that forms at the end of a wing.

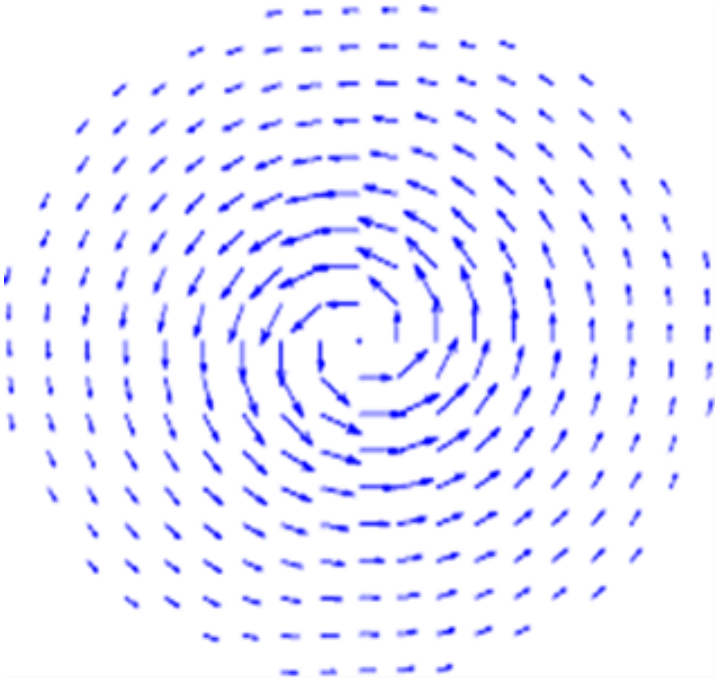

Figure 1.4. Lamb-Oeesen Vortex [10]

1.2.3 Kármán vortex Street

The Karman vortex street is a phenomenon that occurs when a fluid flows past a bluff body, such as a cylinder or a sphere. The fluid flow separates from the surface of the body and forms a series of vortices that alternate in direction. The Karman vortex street is often observed in the wake behind a cylinder and is an important phenomenon in fluid mechanics.

Figure 1.5. Karman Vortex Street [10]

1.2.4 Taylor-Görtler vortex

The Taylor-Görtler vortex is a vortex that is observed in the flow of a fluid between two concentric cylinders that are rotating at different speeds. The Taylor-Görtler vortex is a three-dimensional vortex that has a helical shape and is an important phenomenon in fluid mechanics.

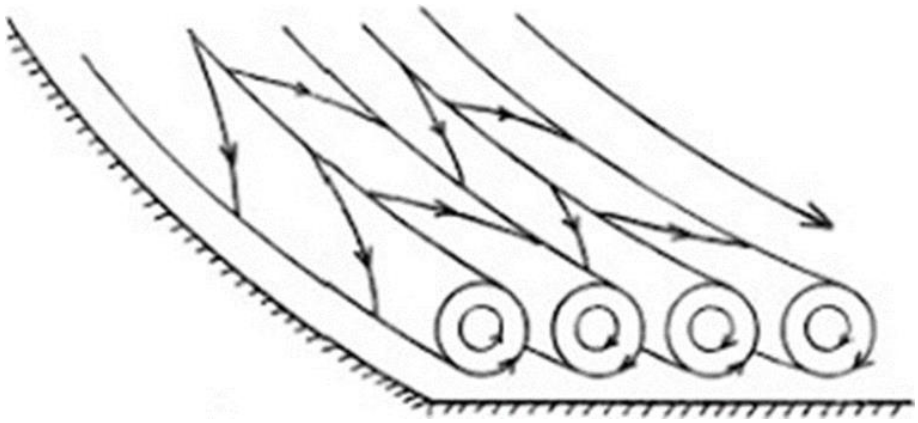

Figure 1.6. Taylor-Görtler vortex [13]

1.2.5 Batchelor Vortex

The Batchelor vortex is a vortex that is observed in a fluid that is rotating uniformly about a vertical axis. The Batchelor vortex is a two-dimensional vortex that has a constant vorticity and is an important phenomenon in fluid mechanics.

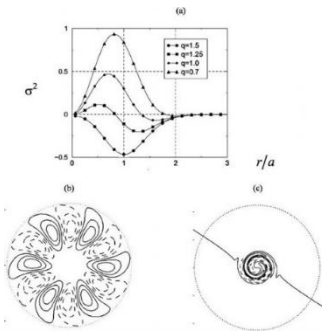

Figure 1.7. Batchelor vortex [14]

1.2.6 Spiral vortex

The spiral vortex is a vortex that has a helical shape and is often observed in the flow around propellers and turbines. The spiral vortex is an important phenomenon in fluid mechanics and is used as a model of vortices that occur in real-life systems such as the flow around at wing tips.

Figure 1.8. Spiral vortex [15]

1.2.7 Wake Vortex

The wake vortex is a vortex that is observed in the wake behind an aircraft. The wake vortex is a three-dimensional vortex that has a complex structure and is an important phenomenon in fluid mechanics. The wake vortex is also a safety concern for aircraft, as it can cause turbulence that can affect other aircraft. Wake vortices are a main set of tip vortices.

Figure 1.9. Wake vortex [16]

1.2.8 Tornado Vortex

The tornado vortex is a vortex that is observed in the atmosphere and is characterized by a rotating column of air that extends from the ground to the clouds. The tornado vortex is an important phenomenon in meteorology and is studied to better understand severe weather events.,

Figure 1.10. Tornado vortex [17]

1.2.9 Oceanic Eddies

Oceanic eddies are vortices that occur in the ocean and are characterized by a swirling motion of water. Oceanic eddies can be observed in a range of sizes, from small-scale eddies that are a few kilometers in diameter to large-scale eddies that are hundreds of kilometers in diameter. Oceanic eddies are an important phenomenon in oceanography and are studied to better understand ocean currents and the transport of heat and nutrients in the ocean.

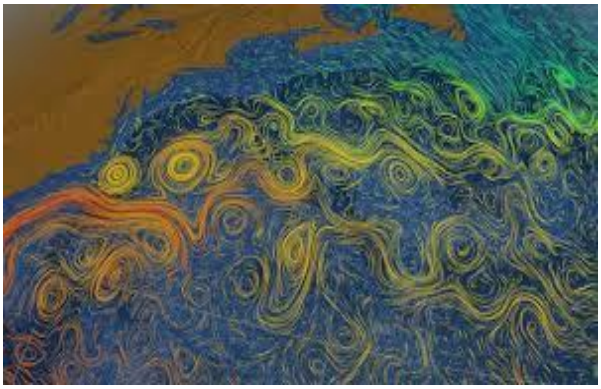

Figure 1.11. Oceanic Eddies [18]

1.2.10 Orszag-Tang Vortex

The Orszag-Tang vortex is a three-dimensional vortex generated from the interaction of two counter-rotating vortices with differing densities and temperatures. Its behaviors is characterized by complexity, including turbulence, instabilities, and other nonlinear phenomena. The properties of fluids are vital in the formation and behaviors of the Orszag-Tang vortex. To comprehend its complex behaviors and the influence of fluid properties, Computational Fluid Dynamics (CFD) simulations are crucial. The insights obtained from studying the Orszag-Tang vortex have various applications in fluid dynamics and Magnetohydrodynamics (MHD) systems.

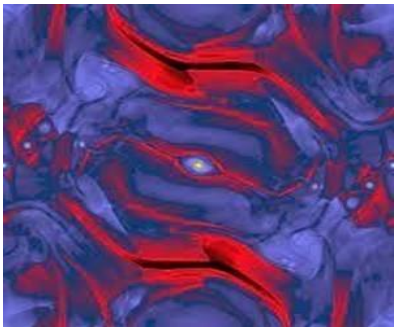

Figure 1.12. Orszag-Tang vortex [19]

1.3 Application of CFD in vortex visualization

Computational Fluid Dynamics (CFD) is a potent instrument for investigating the behaviors of fluid flows, including vortices. Vortices are regions where the fluid rotates around an imaginary axis. They are a common feature in various fluid schemes, from atmospheric flows to industrial processes. CFD simulations enable the visualization and analysis of vortex behaviors in a fluid flow. By numerically solving the governing equations of fluid dynamics, CFD simulations provide detailed information on the velocity, pressure, and other properties of the fluid in and around the vortex. This information can be visualized using streamlines, contours, and vector plots. One of the primary applications of CFD in vortex visualization is the study of turbulent flows. Turbulence is a complex phenomenon characterized by the presence of chaotic, irregular fluid motion. Vortices are a crucial element of turbulent flows, and CFD can simulate and visualize their behaviors, providing insights into the underlying mechanisms of turbulence. CFD simulations can also investigate the effects of different factors on vortex behaviors. Researchers can use CFD to explore the impact of changes in fluid viscosity, temperature, or velocity on vortex formation and evolution. CFD can also study the interaction between vortices and other flow features, such as boundary layers or obstacles, which can significantly impact vortex behaviors. Moreover, CFD simulations can design and optimize fluid schemes, including those involving vortices. By simulating fluid flow behaviors in a virtual environment using CFD, engineers can identify design flaws or inefficiencies and adjust before building the system. This can reduce costs and enhance system achievement. In summary, CFD is a valuable tool for visualizing and analyzing vortices in fluid flows. Its applications range from fundamental research on the dynamics of turbulent flows to the design and optimization of industrial processes that rely on vortices.

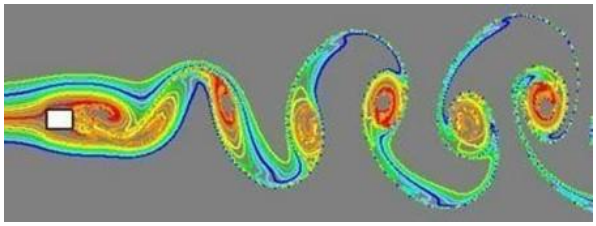

Figure 1.13. CFD applications in industry of fluids [20]

CFD simulations provide a detailed understanding of vortex behaviors and their impact on fluid flows, making it a valuable tool for various scientific and engineering applications [20-21].

The Orszag-Tang vortex is a two-dimensional vortex flow that takes its name from its discoverers. This flow is characterized by the interaction of two counter-rotating vortices that arise in a fluid when it is impulsively initiated. The vortex flow is extensively studied in fluid dynamics research because of its intricate flow features, such as the development of instabilities and the interaction between the vortices. One of the most significant instabilities that can occur in the Orszag-Tang vortex is the Kelvin-Helmholtz instability. This instability is a fundamental phenomenon in fluid dynamics, where shear layers form between two fluids with different velocities. The shear layers can evolve into distinct vortices, creating a turbulent flow. The Kelvin-Helmholtz instability is commonly observed in atmospheric and oceanic flows, as well as in laboratory experiments. The Orszag-Tang vortex is frequently employed as a benchmark problem for testing and validating numerical methods and turbulence models. The vortex's complex flow features make it an excellent test case for evaluating the accuracy and efficiency of computational fluid dynamics (CFD) simulations. Researchers can use CFD simulations to investigate the behaviors of the vortex and its instabilities, providing insights into the underlying mechanisms of turbulence. In addition to the Orszag-Tang vortex, the Kelvin-Helmholtz instability can also occur in other fluid schemes, such as the mixing layer between two parallel streams of fluid. The instability can lead to the formation of complicated flow patterns, including vortices and turbulence. The Kelvin-Helmholtz instability is also a crucial factor in fluid mixing in industrial processes, such as combustion chambers and chemical reactors. Overall, the Orszag-Tang vortex and the Kelvin-Helmholtz

instability are significant topics in fluid dynamics research. These phenomena provide valuable insights into the behaviors of fluid flows and can be used to develop and test numerical methods and turbulence models. Understanding these phenomena is essential for improving our comprehension of real-world fluid schemes, from atmospheric and oceanic flows to industrial processes.

1.4 Properties of fluid importance in 3-D Orszag-Tang vortex

The properties of fluids play a crucial role in Magnetohydrodynamics (MHD), which studies the behaviors of electrically conducting fluids under magnetic fields. The behavior of the fluid is influenced by various properties, including density, viscosity, temperature, and conductivity. Understanding these properties and their interactions with the magnetic field is essential for understanding MHD phenomena and their numerous applications. Density is an important property of fluids in MHD, as it affects the fluid's motion and the strength of the magnetic field. The interaction between the magnetic field and the fluid motion can lead to changes in the density distribution, which can influence the stability and behaviors of the MHD system. Viscosity is another essential property of fluids in MHD, as it determines the resistance of the fluid to shear and deformation. The viscosity of the fluid affects the formation and behaviors of vortices and turbulence, which are crucial phenomena in MHD systems. High viscosity can lead to the suppression of turbulence, while low viscosity can lead to the formation of unstable and chaotic behaviors. Temperature is also an important property of fluids in MHD, as it affects the fluid's conductivity, viscosity, and density. Changes in temperature can lead to changes in the fluid's properties, leading to changes in the behaviors of the MHD scheme. Conductivity is perhaps the most crucial property of fluids in MHD, as it determines the strength of the electric current induced by the magnetic field. The conductivity of the fluid affects the stability and behaviors of MHD schemes, with high-conductivity fluids exhibiting more stable behaviors and low-conductivity fluids exhibiting more chaotic behaviors. In conclusion, the properties of fluids play a crucial role in Magnetohydrodynamics (MHD) schemes.

Understanding the interactions between the magnetic field and fluid properties such as density, viscosity, temperature, and conductivity is essential for understanding MHD phenomena and their numerous applications. MHD simulations provide insight into the behaviors of electrically,conducting fluids under magnetic fields and the influence of fluid properties on MHD behaviors [22-23].

The 3D Orszag-Tang vortex is a classic example of a vortex in fluid dynamics that exhibits complex behaviors. It is a three-dimensional vortex that arises from the interaction between two counter-rotating vortices with different densities and temperatures. The properties of fluids play an essential role in the formation and behaviors of the 3D Orszag-Tang vortex. Density and temperature are two crucial fluid properties that influence the formation and behaviors of the 3D Orszag-Tang vortex. The two counter-rotating vortices have different densities and temperatures, which lead to the formation of a shear layer between them. The shear layer is unstable and causes the formation of smaller vortices that are stretched and twisted by the larger-scale vortices.

Viscosity is another critical fluid property that affects the behaviors of the 3D Orszag-Tang vortex. Higher viscosity leads to more stable behaviors, with less vortex stretching and deformation. Lower viscosity leads to more unstable performances, with more stretching and deformation of the vortices. Conductivity is also an important fluid property in the 3D Orszag-Tang vortex. The presence of magnetic fields can affect the conductivity of the fluid, leading to changes in the vortex behaviors. The interaction between the magnetic fields and the fluid motion can lead to the generation of electric currents, which can further modify the behaviors of the vortex. The 3D Orszag-Tang vortex is a complex phenomenon that exhibits turbulence, instabilities, and other nonlinear behaviors. Understanding the role of fluid properties in the formation and behaviors of the vortex is essential for understanding its complex behaviors. MHD simulations can provide insight into the behaviors of the 3D Orszag-Tang vortex and the influence of fluid properties on its behaviors. In conclusion, fluid properties such as density, temperature, viscosity, and conductivity play a crucial role in the performance of the 3D Orszag-Tang vortex.

These properties influence the formation and behavior of the vortex, including the formation of smaller vortices, stretching and deformation of the vortices, and the generation of electric currents. Understanding the role of fluid properties in the 3D Orszag-Tang vortex is essential for understanding its complex behaviors and has numerous applications in fluid dynamics and MHD schemes [22- 23].

1.5 Importance of Research

Computational Fluid Dynamics (CFD) simulations play a critical role in understanding complex fluid phenomena, including the 3D Orszag-Tang vortex. The 3D Orszag-Tang vortex is a three-dimensional vortex that arises from the interaction between two counter-rotating vortices with different densities and temperatures [24]. CFD simulations provide a detailed understanding of the fluid behaviors and the influence of fluid properties on the vortex formation and performance. One of the primary benefits of CFD simulations is the ability to study the 3D Orszag-Tang vortex in a controlled environment. Researchers can precisely control the fluid properties, basic conditions, and external forces, allowing for the isolation and study of individual factors that contribute to the vortex formation and performance. CFD simulations provide a detailed look at the fluid behaviors, including complex fluid flow patterns that are difficult or impossible to observe experimentally. The visualizations of the fluid flow, including velocity vectors, pressure distributions, and temperature gradients, help researchers understand the complex fluid behaviors and identify patterns and structures in the fluid flow.

In addition to providing visualizations, CFD simulations also provide quantitative data on the fluid behaviors. This data includes vortex strength, deformation, and interaction, which can be used to validate theoretical models and develop new models that accurately describe the fluid behaviors. CFD simulations can also help researchers explore the influence of fluid properties, such as density, temperature, viscosity, and conductivity, on the 3D Orszag-Tang vortex behaviors. By varying these properties schematically, researchers can observe the resulting changes in the vortex behaviors, leading to a better understanding of the role of fluid properties in

the vortex formation and behaviors. In summary, CFD simulations are essential for understanding the 3D Orszag-Tang vortex and other complex fluid phenomena. These simulations provide a controlled environment for studying the vortex behaviors, visualizations of the fluid flow, quantitative data on the fluid behaviors, and the ability to explore the influence of fluid properties. The insights gained from CFD simulations can be used to develop more accurate theoretical models of the fluid behaviors and improve our understanding of fluid dynamics.

1.6 Literature Review

Flint et al. [25] presented an extension of Karlin's entropic lattice Boltzmann (LB) code for Navier-Stokes turbulence to a LB task of magnetohydrodynamics (MHD), incorporating the vector distribution function path of Dellar for the magnetic area. The LB code is analytically decided, and the magnetic area is allowable to own area cancellation. The authors successfully benchmark the limited entropic equation contrary to standard simulations of the Orszag-Tang vortex. This extension of the LB algorithm to MHD is a significant contribution to the area of computational fluid dynamics and may have implications for understanding and predicting the behavior of magnetic areas in turbulent fluids.

Dahlburg et al. [26] presented the outcomes of totally compressible algebraic simulations of the Orszag-Tang vortex case using Fourier collocation. The scheme is initialized with a non-random, periodic area containing X points in velocity area besides magnetic area, however with different process structures along a dimensional direction. The introductory velocity area is solenoidal, and the introductory pressure area is a superposition of convenient incompressible pressure disposal and a flat pressure area resembles the introductory enrage Mach number of the flow. The authors differ the introductory Mach number up 0.2 to 0.6, corresponding to enrage plasma beta values differs from 30.0 to 3.3, appropriately. It is revealed the raise of compressible possessions within one or two Alfvén passage times, as proved by the range of compressible portions such as mass density and non-solenoidal flow area, by simulations. These effects include a retardation of growth of correlation between

the magnetic area and velocity area, the evolution of compressible small-range structures such as heavy jets, and bifurcation of eddies in the compressible flow.

The data suggest that, when enrage Mach number increases, the gap between incompressible and compressible results increase. The study provides valuable insights into the behavior of compressible fluids and may have implications for understanding and predicting the behavior of plasma in astrophysical environments.

Dudson et al. [27] simulated complex fluid behavior and instabilities in tokamaks is crucial for the development of nuclear fusion as an energy source. Over the years, various numerical codes have been developed to model magnetohydrodynamic (MHD) processes in tokamaks such as the Edge Localized Modes (ELMs). These codes solve the MHD equations in various geometries and have helped gain valuable insights into plasma instabilities in tokamaks. A new code called BOUT++ presented by [author name] aims to simulate 3D fluid equations in curvilinear geometries, especially to study ELMs in x-point tokamak geometry. The code is highly modular and can simulate a big range of fluid models in arbitrary geometries. It uses a fully implicit time evolution method and third order WENO schemes for higher accuracy. The code has been benchmarked with linear and nonlinear test cases such as the Orszag-Tang vortex, showing good agreement with theoretical and experimental results. BOUT++ also shows good scalability on high- achievement computing systems, indicating its capability for large-scale, high- resolution simulations. Overall, BOUT++ adds to the current repertoire of numerical tools for studying plasma fluid instabilities and turbulence in magnetic confinement fusion devices like tokamaks. Its modularity and computational efficiency make it suitable for simulating a big range of phenomena. Studies done using the BOUT++ code would provide valuable contributions towards the understanding and control of ELMs and other MHD instabilities in tokamaks.

Huazheng et al. [28] showed a new hybrid numerical scheme that combines the Energy-Convective Upwind and Split Pressure (E-CUSP) method for the fluid part with the Constrained Transport (CT) method for the magnetic induction part to simulate magnetohydrodynamic (MHD). To avoid negative pressure in the

reconstructed profiles, a positivity preserving method is introduced. Additionally, the MHD equations are solved at each physical time step byadvancing in pseudo time. The use of dual time stepping allows the physical time step to be selected based on the numerical accuracy criterion, rather than being limited by the smallest cell size. The achievement of the planned hybrid scheme is reached using benchmark problems, including the 3D Orszag-Tang vortex problem and the 2D shock-cloud interaction case, demonstrating its accuracy and robustness. The planned hybrid scheme may provide a more efficient and accurate approach for simulating MHD problems, making it a significant contribution to the field of computational fluid dynamics.

Feng et al. [29] introduced the rotated-hybrid scheme for 3D magnetohydrodynamics (MHD) equations in the finite-volume frame for the first time. The scheme is based on decomposing a cell-face normal vector into two orthogonal directions and combining the Roe solver, a full-wave or complete Riemann solver, and the Rusanov solver, an incomplete Riemann solver, into one rotated-hybrid Riemann solver. To preserve the divergence-free nature of the magnetic area, two divergence-cleaning approaches are proposed by combining the least-squares reconstruction of the magnetic area with the divergence-free constraints.

One approach is focused on locally maintaining the magnetic solenoidality exactly, while the other is globally solenoidality-preserving (SP) and is implemented by adding a global constraint. Both SP methods are implemented to 3D MHD with a rotated-hybrid scheme in the finite- volume frame. To validate and demonstrate the capabilities of the rotated-hybrid scheme for MHD, the authors perform an Orszag-Tang MHD vortex case and a numerical study of the steady-state coronal structures of Carrington rotation 2068 during the solar activity minimum. The numerical tests demonstrate the robustness of the planned scheme and the capability of the SP approaches to keep the magnetic divergence errors within the expected accuracy. The rotated-hybrid scheme and the proposed SP approaches may provide a more efficient and accurate approach for simulating MHD problems in various applications, such as astrophysical fluid dynamics and plasma physics.

Feng et al. [30] proposed a new numerical scheme that combines the Energy-Convective Upwind and Split Pressure (E-CUSP) method with the Constrained Transport (CT) method for simulating magnetohydrodynamic (MHD) problems. The scheme, which follows the work by Shen et al. (2012), uses the Ziegler CT method for the magnetic induction part. To avoid negative pressure in reconstructed and updated profiles, a mixed method of positivity preserving method is employed. Additionally, the MHD equations are solved at each physical time step by advancing in pseudo time. The planned scheme is reached through numerical experiments of benchmark problems, including the 2D Orszag-Tang vortex case and the 3D blast wave case, demonstrating its accuracy and robustness. The results suggest that the planned scheme may provide a more efficient and accurate approach for simulating MHD problems in various applications, such as astrophysical fluid dynamics and plasma physics. This contribution is significant to the field of computational fluid dynamics, particularly for those working on MHD simulations.

Jiang [31] presented a high-order accurate weighted essentially non-oscillatory (WENO) finite difference scheme for solving the equations of ideal magnetohydrodynamics (MHD). The WENO scheme is a direct extension of a successful scheme applied to hydrodynamic problems, and it achieves higher-order accuracy with fewer computations. Both ENO and WENO can be easily applied to two and three spatial dimensions. The authors present details of the WENO scheme and the construction of a suitable eigen-scheme, which can properly decompose various families of MHD waves and handle degenerate situations. Numerical results demonstrate the scheme's achievement for the one-dimensional Brio-Wu Riemann problems, the two-dimensional Kelvin-Helmholtz instability problems, and the two-dimensional Orszag-Tang MHD vortex system. The importance of maintaining the divergence-free condition for the magnetic range in achieving numerical stability is highlighted. The tests also show the advantages of using the higher-order scheme, as the new 5th-order WENO MHD code can attain accuracy comparable with that of the second-order schemes with many fewer grid points. This contribution may provide a more efficient and accurate approach for simulating MHD problems in various applications, such as astrophysical fluid dynamics and plasma physics. The

article is significant to the area of computational fluid dynamics, particularly for those working on MHD simulations.

Armstrong et al. [32] discussed the role of viscous effects in the energy release mechanisms of solar flares. The authors investigate the contribution of viscous dissipation in current-sheet reconnection solutions using side-by-side planar reconnection simulations. The simulations are driven by the Orszag-Tang vortex, and the authors utilize both classical and Braginskii forms of viscosity to provide an autonomous MHD scheme that develops strong current layers sustained by large-scale vortical shearing flows. Analytical scaling laws are used to determine the dissipation rates, which suggests that viscous losses generated from large-scale non-uniform velocity areas are likely to dominate resistive losses. The findings of this study provide insight into the role of viscous effects in reconnection and energy release mechanisms in solar flares. However, further research is needed to understand the broader implications of these findings for more general merging situations.

Snow et al. [33] discussed the occurrence and classification of shocks in compressible magnetohydrodynamic (MHD) turbulence, which is a common feature of astrophysical schemes such as the solar atmosphere and interstellar medium. The authors present a method for detecting and classifying the full range of MHD shocks using the Orszag-Tang vortex as a test case. The study reveals that the scheme is dominated by fast and slow shocks, with intermediate shocks appearing less frequently, particularly near magnetic reconnection sites. The authors also propose a potential mechanism for the formation of intermediate shocks in MHD schemes. The findings of this study provide insights into the coherency and abundances of shocks in compressible MHD turbulence and shed light on the role of shocks in redistributing and dissipating energy in astrophysical schemes. However, further research is needed to understand the broader implications of these findings for other astrophysical schemes and to assess the impact of shock-dominated turbulence on the evolution and dynamics of these schemes.

Tu[34] discussed the development of a meshless method for magnetohydrodynamics (MHD) that evolves the vector potential of magnetic range. The authors propose a novel scheme and numerical techniques to restrict the divergence of magnetic area based on the Meshless Finite Mass/Volume with HLLD Riemann solver for conservative flux calculation. The study shows that the magnetic field can be stabilized by a proper smoothing process, making long-term evolution possible. To validate the new scheme, the authors perform various test cases, including the Brio-Wu shock tube, 2D and 3D Orszag-Tang vortex, and Magneto rotational Instability. The results demonstrate that the planned method is robust and has better precision on central offset, amplitude, and detailed patterns than an existing meshless code, GIZMO. The findings of this study provide a promising approach to solving MHD cases without the need for a mesh, which can be particularly useful for cases involving complex geometry or astrophysical systems. However, further research is needed to assess the broader implications of these findings and to compare the achievement of the planned method with other MHD solvers.

Cartes [35] discussed the derivation of new generalized equations of motion for Weber-Clebsch potentials that describe both Navier-Stokes and magnetohydrodynamics (MHD) dynamics. The new equations depend on a new parameter that has dimensions of time for Navier-Stokes and inverse velocity for MHD. Direct numerical simulations are performed to validate the new formalism. For Navier-Stokes, the simulations capture the intense reconnection of vortices of the Boratav, Pelz, and Zabusky flow, consistent with previous studies. For MHD, the new formalism is used to detect magnetic reconnection in various flows, including the three-dimensional Arnold, Beltrami, and Childress flow and the two-dimensional and three-dimensional Orszag-Tang vortex. The study concludes that periods of intense activity in the magnetic entropy are correlated with periods of raising, frequent resetting and discusses the positive correlation between the sharpness of the increase in resetting frequency and the spatial localization of the reconnection region. The findings of this study provide a promising approach to understanding the dynamics of Navier-Stokes and MHD systems and could have significant implications for the study of astrophysical schemes. However, further

research is needed to validate the new formalism for a broader range of cases and to assess its performance compared to other existing methods.

Jadhav [36] investigated direct numerical simulations of magnetohydrodynamic turbulence with Orszag-Tang vortex basic conditions for two different Reynolds numbers. The simulations are carried out using a pseudo- spectral code with a grid resolution fine enough to resolve the Kolmogorov scale. The study analyzes the power-law behavior of bulk quantities such as kinetic energy, magnetic energy, integral length scales, and entropy. For a low Reynolds number, weak turbulence spectra with a slope of -2.0 in the inertial subrange are observed, while for a higher Reynolds number, the spectra exhibit a slope very close to the Kolmogorov spectra of -5/3. The Q-criteria iso-surfaces are used for the visualization of turbulence developed within the flow at the time instant of maximum entropy. Additionally, a new approach is presented to understand the dynamics of the transfer between kinetic and magnetic energies in the early period of development using the energy flux spectra, rate of change of kinetic and magnetic energies, and current density structures. The study employs a three- dimensional representation of the alignment between velocity and magnetic field across the structures. The findings of this study provide insights into the dynamics of Orszag-Tang vortex turbulence and the transfer of energy between kinetic and magnetic forms. However, further research is needed to validate these findings for a broader range of cases and to assess their implications for the understanding of astrophysical scheme.

CHAPTER 2

METHODOLOGY

2.1 Problem Description

In computational fluid dynamics (CFD), the Orszag-Tang vortex presents a classic case that involves simulating a complex, three-dimensional, incompressible flow. The vortex is named after William T. Orszag and Shu-Cheng Tang, who first described it in 1979. The Orszag-Tang vortex consists of two counter-rotating vortices generated by the interaction of two sinusoidal velocity perturbations imposed on a uniform flow. The resulting flow field exhibits complex phenomena such as turbulence, shock waves, and vortex interactions, making it a challenging problem for CFD simulations. The primary objective of simulating the Orszag- Tang vortex is to gain a better understanding of the underlying physics of complex fluid flows and to develop and test numerical methods for solving the Navier- Stokes equations that govern fluid behaviors. This case is often used as a benchmark to assess the accuracy and efficiency of CFD codes and numerical algorithms. Even though it is a two-dimensional case, the Orszag-Tang vortex displays many of the characteristics of three-dimensional flows, making it a valuable test case for developing and validating numerical methods for simulating more complex fluid flows. The case has been extensively studied over the years, leading to the developing and validating numerical methods for simulating more complex fluid flows.

2.2 CFD with OpenFOAM

OpenFOAM is a software package used in computational fluid dynamics (CFD) to solve partial differential equations governing fluid flow using finite volume methods. It offers a big range of pre-processing, solver, and post-processing capabilities,

making it a versatile tool for simulating complex fluid flows. OpenFOAM is an open-source software package, allowing users to modify and customize its code to meet their specific needs. This flexibility enables users to tailor the software to their own requirements in research, industry, or academia. Additionally, OpenFOAM has a robust user community and extensive documentation, making it accessible to users of all levels, from beginners to advanced users.

As it can be seen from figure the program works in three steps pre-processing includes utilities and meshing tools.The constant folder includes mesh and geometry properties. Meshing is so easy because the one can create own geometry by entering points then determine surfaces and finally by combining the surfaces volume can be done, in addition meshes are always include structured grides.

Second step is solution step everything designed by users, modify of basic folders the program includes like system and zero folders. The last step post-processing contains visualization part by using ParaView.

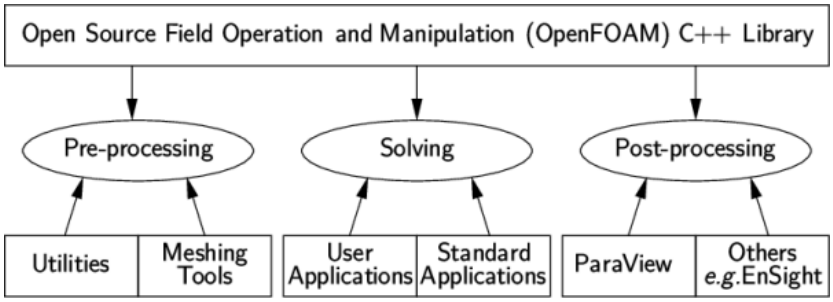

Figure 2.1. OpenFOAM C++ Library [45]

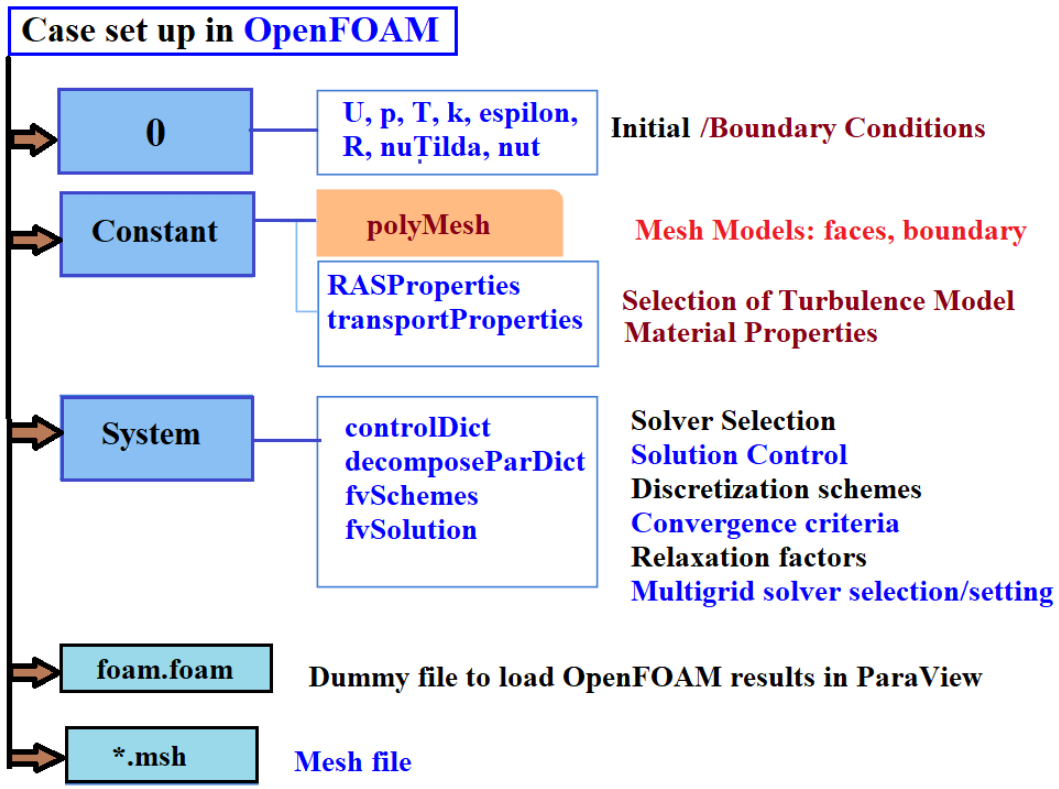

Figure 2.2. OpenFOAM case structure

To design a flow simulation, OpenFOAM needs 3 distinct folders which are system/constant/ and 0/ respectively. The file structure of an OpenFOAM case file is given in Figure 3.2.2 The system/ folder and files under includes the knowledge about the numerical method and input/output context for the essentials. In the constant folder settings are determined related to the pathway territory and the fluid(s) to be flow with.

In 0/ folder, boundary conditions for the cases are given dispereteley for any flow variable. Fundamental case folders and files under for an OpenFOAM simulation are given in a more accurate sense below:

- System/: contains controlDict, fvSchemes and fvSolution files

– controlDict: In this file, input/output and time step parameters such as which solver to use,time step period, output period pertime step, start-finish times of

thesimulation, etc .. are described. These libraries generally generated by users which can be used in the simulation of new design.

– fvSchemes: In this file, numerical design to be used in the solver are given absolutely similarly using which numerical design to work out laplacian of P, gradient of U, etc ..

– fvSolution: Solver parameters such as convergence standards, degree of freedom factors for variables, etc .. are defined in this file.

• Constant/: This folder consist of transportProperties, turbulenceProperties files besides polyMesh folder:

– transportProperties: At the part of file, the physical properties belongs to the

fluid worked with such as kinematic viscosity, dynamic viscosity, heat capacity are concluded.

– turbulenceProperties: Selection of the turbulence model is done in the file to be used and describe the coefficients for the turbulence model.

– polyMesh/ folder: The reservation of data associated to the solution domain and its mesh take place in distinct files like points, edges, f aces, cells and boundaries.

• 0/: In this folder, boundary and initial conditions for any variable flow variable are described in different files like (p, U, B etc.). [46]

The software package includes solvers for various types of fluid flows, including laminar and turbulent flows, compressible and incompressible flows, and single- and multi-phase flows. Furthermore, OpenFOAM supports a range of boundary conditions, such as inflow, outflow, wall, and symmetry conditions, which can be customized to suit specific applications. OpenFOAM provides pre-processing tools for setting up and meshing the computational domain and post-processing tools for visualizing and analyzing simulation results. The software supports a range of file formats, including its own format as well as STL and VTK, allowing users to import and export data between different software packages. In conclusion, OpenFOAM is

a powerful and versatile tool used to simulate complex fluid flows in various areas, including engineering, physics, and environmental sciences. Its open-source nature, user community, and extensive documentation make it a popular choice for researchers, students, and practitioners in the field of CFD [37- 38]. Moreover, RAS type turbulence model k- Epsilon one used in the study.

2.3 RANS Turbulence Model

Turbulent flow is described as an unsteady folw field results in upredicted, irregular motion besides three dimensional velocity in flow area. To predict the irregular motion in literature different types of turbulancce models are defined. These are: LES (Large Eddy Simulation), Detached Eddy Simulations (DES), (U)RANS equations: (Unsteady) Reynolds Time Averaged Navier-Stokes equations, Direct Numerical Simulations (DNS)

All turbulent length ranges are simulated in RANS. It has been the pathway for the following.

Century in modern CFD method for simulating the turbulent flow due to it requires low- cost buget for computing necessities and economical to get. The analysis is pricipally focused with the most common low Reynolds number k−ε turbulence models for such computer guessing in computing turbulence flows. The advantages of low Reynolds number k−ε turbulence models over standard models (k -w and k-ε) are that it needs less number of mesh points, represents the adequately well set up near-wall distribution which lowering mesh sensitivity The k-w model handle the turbulance according to the turbulence frequency of the large eddies.

It is used that both parameter the dissipation rate of turbulance kinetic energy (ε) and specific dissipation rate (k) to derive two transport equations for turbulance equations [46-47].

Standard κ- ε Model

Turbulent Kinetic Energy

$$\rho U_i \frac{\partial k}{\partial x_i} = \mu_i \left(\frac{\partial U_j}{\partial x_i} + \frac{\partial U_i}{\partial x_j}\right)\frac{\partial U_j}{\partial x_i} + \frac{\partial}{\partial x_i}\left\{(\mu_1/\sigma_k)\frac{\partial k}{\partial x_i}\right\} - \rho\epsilon \quad . (2.1)$$

Dissipipation Rate

$$\rho U_i \frac{\partial k}{\partial x_i} = C_{1\varepsilon}\left(\frac{\varepsilon}{k}\right)\mu_1 \left(\frac{\partial U_j}{\partial x_i} + \frac{\partial U_i}{\partial x_j}\right)\frac{\partial U_j}{\partial x_i} + \frac{\partial}{\partial x_i}\left\{(\mu_1/\sigma_\varepsilon)\frac{\partial \varepsilon}{\partial x_i}\right\} - C_{2\epsilon}\rho\left(\frac{\varepsilon^2}{k}\right) \quad (2.2)$$

where σ_k, σ_ε, $C_{1\varepsilon}$, $C_{2\varepsilon}$ are empirical constants and these equations written for steady, incompressible flow.

2.4 Governing Equations

To have a mathematical model of a compressible MHD fluid eight PDE's are required which are combination of Navier-Stokes and Maxwell's equation of electromagnetics. According to the ideal MHD the main opinion to get expanded spectrum of discontinuites especially the resistive and diffusive terms explaining the viscous and magnetic stress tensors. Moreover,energy loss because of mechanical stresses and the joule heated are neglected. Thus, in terms of above conditions assumption of ideal conducting plasma term can be mentioned. Ideal MHD equations comes from conservation of mass, three momentum equations, three equations comes from induction of magnetic field and energy equation. Final equation is about divergence cleaning method implement to get accurate results.

In this part of thesis, we used the ideal magnetohydrodynamics governing equation which was solved in OpenFOAM software. Both fluid and electromagnetic component of present work has been showed in below [39-40].

$$\frac{\partial}{\partial t}(\rho) + \nabla(\rho u) = 0 \quad (2.3)$$

$$\frac{\partial}{\partial t}(\rho u) + \nabla\left(\rho uu + I(p + \frac{BB}{2})\right) - BB = 0 \quad (2.4)$$

$$\frac{\partial}{\partial t}(B) + (uB - Bu) = 0 \quad (2.5)$$

$$\frac{\partial}{\partial t}(\rho e) + \nabla\left(\rho e + p + \frac{BB}{2}\right)u - B(uB) = 0 \quad (2.6)$$

Magnetic field constraint called as Gauss law of magnetism like

$$\nabla B = 0 \tag{2.7}$$

The unknown ρ is called density of fluid, u and B are velocity and magnetic field vectors in three dimension like (u,v,w) and (B_x , B_y , B_z) respectively.Furthermore, p is static pressure, p_t is total pressure which is summation of static and magnetic pressure, e is the total energy per unit mass and I is an identity tensor.

$$p_t = p + \frac{1}{2}\left(B_x^2 + B_y^2 + B_z^2\right) \tag{2.8}$$

Here is the total energy is:

$$\rho e = \frac{1}{2}\rho u^2 + \frac{1}{2}B^2 + \frac{p}{(\gamma - 1)} \tag{2.9}$$

$$\rho e = \frac{1}{2}\rho(u^2 + y^2 + z^2) + \frac{1}{2}\left(B_x^2 + B_y^2 + B_z^2\right) + \frac{p}{\gamma - 1} \tag{2.10}$$

2.4.1 Derivation of Ideal Magnetohydrodynamics Equations

Derivation of Ideal MHD equations done with combination of Maxwell's equations and Navier-Stokes Equations.

$$\nabla \times \vec{E} = -\frac{\partial B}{\partial t} \quad \text{(Faraday's Law)} \tag{2.11}$$

$$\nabla \times \vec{B} = \mu_0 \vec{J} + \frac{1}{c^2}\frac{\partial \vec{E}}{\partial t} \quad \text{(Ampere's Law)} \tag{2.12}$$

$$\nabla . \vec{E} = \frac{\rho_c}{\epsilon_0} \quad \text{(Gauss' Law for Electricity)} \tag{2.13}$$

$$\nabla . \vec{B} = 0 \quad \text{(Gauss' Law for Magnetism)} \tag{2.14}$$

Where ρ_c = e (n_e- z n_i) (charge density) (2.15)

ρ_C is charge density, e is charge of an electron, n_e is number of density of an electron, z is charge of an ion, n_i is number of ion density.

Maxwell equations have two non-relavitistic limits (v$\ll c$) which is magnetically dominated (v$\ll$c , E$\ll c.B$) and this case is used in astrophysics at most.

Moreover, (v$\ll$c , E$\gg c.B$) which is electrically dominated and this condition used in daily life cases at most.

In the magnetically dominated limit displacement current can be neglected;

$$\nabla \times \vec{E} = -\frac{\partial \vec{B}}{\partial t} \quad (2.16)$$

$$\nabla \times \vec{B} = \mu_0 . \vec{j} \quad (2.17)$$

Transport into co-moving frame using the equation:

$$\vec{E}' = \vec{E} + \vec{v} \times \vec{B} \quad (2.18)$$

$$\vec{B'} = \vec{B} \quad (2.19)$$

By the frame relation between $\vec{E}$ and $\vec{j}$ can be supported via Ohm's Law.

$\vec{j'} = \sigma \vec{E'}$ like V= $I.R$

where σ is electrical conductivity, j is magnetic current, ϵ_0 is magnetic permitivity and μ_0 is magnetic permeability.

Equivalently, assumed that $\rho_c{}' = 0$ means charge neutrality in co-moving frame is implies $\vec{E'} = 0$ in referance of Gauss' Law for Electricity.

$\vec{E'} = \frac{\vec{j'}}{\sigma} = 0$ if $\sigma \to \infty$ which means infinite conductivity.

When the co-moving frame also implemented on Faraday's Law:

$$\frac{\partial \vec{B}}{\partial t} = -\nabla \times \vec{E'} + \nabla \times \left(\vec{v} \times \vec{B}\right) \quad (2.20)$$

$$\frac{\partial \vec{B}}{\partial t} = -\nabla \times \left(\frac{\vec{j'}}{\sigma}\right) + \nabla \times \left(\vec{v} \times \vec{B}\right) \text{ or } \frac{\partial \vec{B}}{\partial t} = \nabla \times \left(\vec{v} \times \vec{B}\right) - \nabla \times \left(\eta \nabla \times \vec{B}\right) \quad (2.21)$$

Where $\eta = \frac{1}{\sigma \mu_0}$ means resistivity and for a perfect conductor $\sigma \to \infty$ then $\eta \to 0$.

$$\frac{\partial \vec{B}}{\partial t} = \nabla \times \left(\vec{v} \times \vec{B}\right) \quad (2.22)$$

Fluid equations are usual but with Lorent'z force:

$$\vec{F} = q\left(\vec{E} + \vec{v} \times \vec{B}\right) \quad (2.23)$$

$\vec{J} = \rho_c \vec{E} + \rho_c \vec{v} \times \vec{B}$ because $\rho_c \vec{E}$ term goes to zero and $\rho_c \vec{v} = \vec{J_c}$, (current) then

$$\vec{j} = \vec{J} \times \vec{B} \quad (2.24)$$

$\frac{d\rho}{dt} = -\rho(\nabla \vec{v})$ also $\frac{d}{dt} = \frac{\partial}{\partial t} + \vec{v}.\nabla$ the rule can be applied to conservation of mass equation.

$\frac{d\vec{v}}{dt} = -\frac{\nabla p}{\rho} + \frac{\vec{J} \times \vec{B}}{\rho}$ is momentum equation with magnetic force. (2.25)

$$\frac{d\vec{u}}{dt} = -\frac{\mathrm{p}}{\rho}(\nabla \vec{v}) \quad (2.26)$$

$$\frac{d\vec{B}}{dt} = \nabla \times \left(\vec{v} \times \vec{B}\right) \quad (2.27)$$

$\nabla \times \left(\vec{v} \times \vec{B}\right) = \left(\vec{B} \,.\nabla\right)\vec{v} - (\vec{v} \,.\nabla)\vec{B}$ is an anti-symmetric equation. (2.28)

$$\frac{d\vec{B}}{dt} = (\vec{B} \,.\nabla)\vec{v} - \vec{B}\,(\nabla.\vec{v}) \quad (2.29)$$

These governing equations are describe behaviour of conducting fluids according to magnetic field. MHD equations derived from Maxwell's equations of electrodynamics and Ohm's law, matched with the momentum equation for incompressible fluid. Final form of MHD equations for incopressible laminar flow used in Pietersen's work [40] are like that:

$$\frac{\partial \vec{B}}{\partial t} = \nabla \times \left(\vec{u} \times \vec{B}\right) - \frac{\nabla \times (\vec{j})}{R_m} \quad (2.30)$$

$$\frac{\partial \vec{u}}{\partial t} = \vec{j} \times \vec{B} - (\vec{v}.\nabla)\vec{u} + \nabla^2\,(\vec{v}.\vec{u}) \quad (2.31)$$

$$\nabla.\vec{B} = 0 \quad (2.32)$$

$$\nabla.\vec{u} = 0 \quad (2.33)$$

Here, B is the magnetic area, u is the velocity area, the current density j is givenby $\vec{j} = \nabla \times \vec{B}$ and Rm is the magnetic Reynolds number, further will be explained below. In this thesis, the OpenFOAM software used to investigate the property of fluids properties, Reynolds number and etc.

The ordinary Reynolds number, which: indicates the degree of turbulence in a fluid, is defined as:

$$\dot{Re} = \frac{1}{\vartheta} \tag{2.34}$$

Where ν is the kinematic viscosity. This parameter is significant for any CFD simulation since turbulence has a strong influence on computational and dynamical properties. The OpenFOAM packages used in this study assume laminar flow, so Reynolds numbers in the considered cases must be low enough. In this study, all cases considered have Re ≤ 50, well below the critical Reynolds number of most geometries, including the ones considered in this study. Motivated by the Reynolds number, magnetohydrodynamics is also characterized by the magnetic Reynolds number. This number is a measure for the magnitude of the induced field relative to the inducing field. It is defined as follows:

$$\sigma = \frac{1}{\mu\lambda} \tag{2.35}$$

Where σ is the electrical conductivity, λ is the magnetic diffusivity, and μ is the magnetic permeability. U and L are typical velocity and length scales, respectively. In this study also Pietersen's work is main referance while equations and parameters are similar in these works of Tóth, Wang,Yalim, and Balasubramanian [40-44] those assume μ = 1 for plasma, and in the cases studied, the case have

$$U.L = 1 \tag{2.36}$$

The ratio of Lorentz force to viscous force is captured by the Hartmann number Ha, which is defined as:

$$Ha = B.L.\sqrt{\frac{\sigma}{\mu}} \tag{2.37}$$

CHAPTER 3

COMPUTATIONAL TEST CASE
ORSZAG-TANG VORTEX

3.1 Orszag-Tang Vortex Problem Description

In this part of thesis, after analyzing the 3D Orszag-Tang vortex importance in fluids mechanics in chapter one, and literature review analyzing had been done in chapter two. In chapter three, we focused on validation of results, mesh, and time step independent test, we introduced the methodology. In this chapter we focused on the results of results and considered the effects of various parameters on 3D Orszag-Tang vortex.

3.2 Grid Independence Study

Computational fluid dynamics (CFD) boundary conditions play a crucial role in determining the accuracy and reliability of the simulation of a Orszag-Tang vortex. The boundary conditions define the behaviors of the fluid at the boundaries of the simulation domain and are used to simulate the flow of air in Orszag-Tang vortex. The boundary conditions that need to be defined for an Orszag-Tang vortex simulation include the cyclic walls boundary conditions. The main part of the present simulation is considering the initial values for velocity and electromagnetic fields. We used code stream of OpenFOAM to capture the initial values of velocity and electromagnetic areas. All mentioned boundary conditions have been shown in the table.

Table 3.1. Boundary conditions

Boundary	Pressure	Magnetic Area	Velocity
Walls	Cyclic	Cyclic	Cyclic
Initial	Cyclic	β (-2 sin y+ sin z, 2 sin x +sin z , sin x + sin y)	(-2 siny, 2sinx, 0)

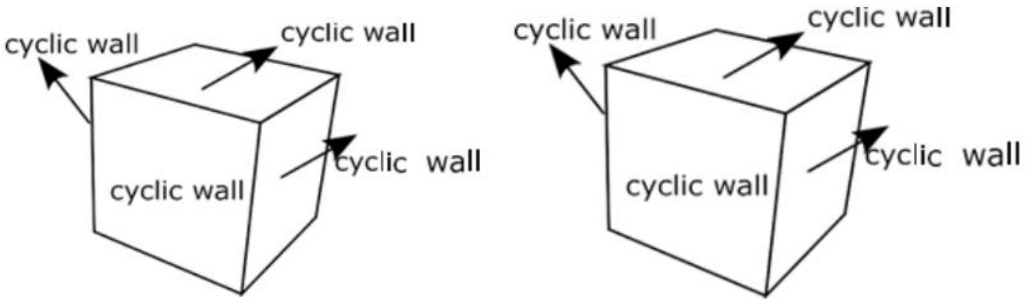

Flow goes through one neighbor surface to other and it is assumed that the motion repeated to provide the condition of continuous flow.

3.2.1 Initial Conditions

The Orszag-Tang vortex is a well-known fluid dynamics phenomenon that occurs when two fluids with different densities and velocities are brought into contact. This creates a series of vortices that interact with each other and cause complex fluid dynamics behavior. Additionally, electromagnetic areas can be introduced to the system, leading to what is known as magnetohydrodynamics (MHD). When an electromagnetic area is applied to an Orszag-Tang vortex, the flow behavior changes because of the interaction between the fluid and the magnetic field. This interaction can lead to the formation of current sheets, which in turn can cause magnetic reconnection and energy release. The resulting behavior is highly complex and depends on a variety of factors, including the strength of the magnetic field, the

density of the fluid, and the velocity of the fluid. The interaction between the Orszag-Tang vortex and the electromagnetic area has important implications for a variety of scientific and technological fields. For example, understanding the behavior of MHD schemes is crucial for developing more efficient fusion reactors and for studying the dynamics of astrophysical phenomena such as solar flares and coronal mass ejections.

Additionally, MHD schemes are important in the study of geophysical phenomena such as the Earth's magnetic field and the behavior of the Earth's ionosphere. Overall, the interaction between the Orszag-Tang vortex and fluid flow and electromagnetic fields is a complex and fascinating area of study with important implications for a variety of scientific and technological areas. The mhdFoam solver is a laminar incompressible MHD solver, based on the momentum equation for incompressible fluids and the coupled Maxwell-Navier stokes equations. First the solver sets up the linear algebra for the U equation.

The solver then predicts U with the so called “momentum predictor”, $-\nabla p$ at line12. Figure 3.4 of codes takes place in appendix. The solver then enters a PISO loop, that solves the momentum equation ”UEqn” up to the desired tolerance specified in system/fvSolution. In this study, this is always 10^{-5} for all fields - U, B, B_t and B_{fixed} except for the pressure field, which has a tolerance of 10^{-6} For further details of the PISO algorithm, the reader is referred to the online documentation provided by OpenFOAM.

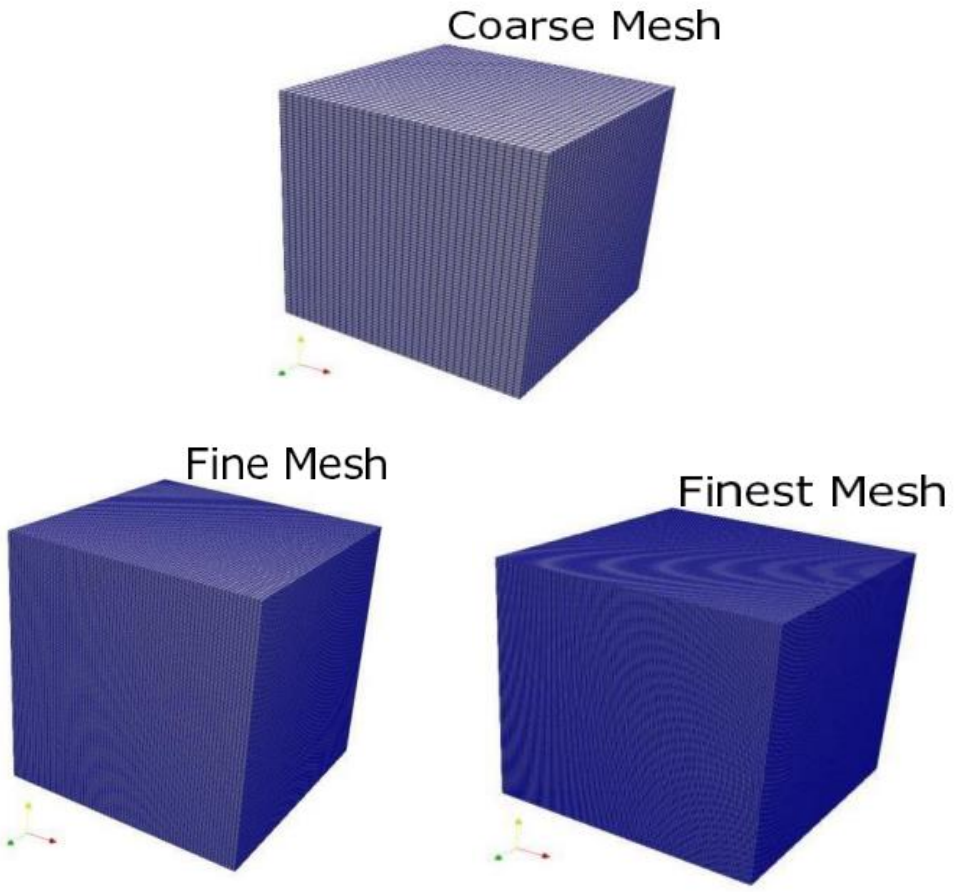

Figure 3.1 Various meshes of present work and schematic view.

3.3 Time Step Size Study

The present section of the thesis investigates a numerical method for creating an Orszag-Tang vortex using computational fluid dynamics (CFD). To accomplish this, open-source software such as OpenFOAM is utilized. The first step in this approach is to build a 3D model of the Orszag-Tang vortex, which includes the cyclic wall and predetermined basic values for electromagnetic and velocity distributions. OpenFOAM is then used to set up the simulation by defining the boundary conditions, fluid properties, and solver settings, which captures the flow of air through the Orszag-Tang vortex domain. The simulation is then executed, producing data that can be used to examine the Orszag-Tang vortex behaviors. The mhdFoam

solver is used in this investigation to analyze the Orszag-Tang vortex. This numerical approach yields a precise analysis of the Orszag-Tang vortex behaviors, ensuring that it complies with design requirements. Figure 3.4 depicts a schematic view of the Orszag-Tang vortex, while Table 3.4 provides its dimensions. In this study, the 3D Orszag-Tang vortex was examined using timestep $\Delta t = 0.00001$ and various grids.

Table 3.2 Dimensions of Maisotsenko cycle heat exchanger

Characteristics	H	L	W
Value	2π	2π	2π

The mesh was set up using Open Foam's integrated block Mesh utility, with simple Grading (1 1 1), i.e. with an expansion ratio of 1 in x, y and z direction. The basic profiles for velocity and magnetic area are set using the code stream utility. Transport variables are set equal to $\mu = \rho = 1$, while ν and λ are set equal to 0.02, implying Re = Rm = 50.

Upon analyzing the time step, our findings indicate that a time step of 10^{-5} s is good enough for the present temporal accuracy for the current study. Both 10^{-5} s and 10^{-6}s consistent through the time independent test for Orszag-Tang vortex problem.

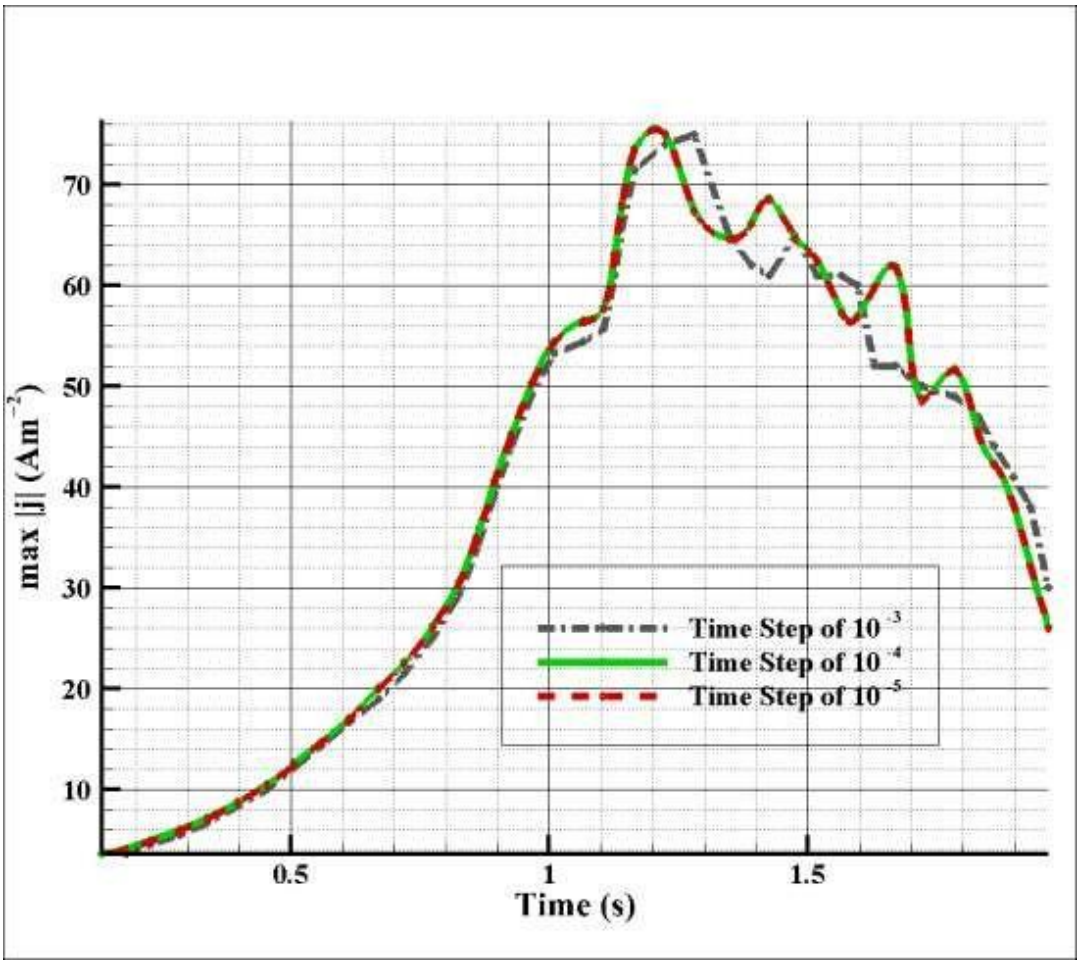

Figure 3.2 Time independent test for Orszag-Tang vortex problem

In the context of Computational Fluid Dynamics (CFD), a timeindependent test refers to a simulation or analysis in which the flow conditions and parameters are assumed to remain constant over time. This type of test is often used to evaluate the steady-state behavior of a fluid flow within a given system. In CFD, engineers and researchers often use time-independent simulations to study the flow patterns, pressure distributions, and other characteristics of a fluid within a specific geometry or environment. These simulations are particularly useful for understanding the behavior of fluid systems under steady-state conditions, where the flow variables do not change with time. Time-independent tests in CFD involve solving the governing equations of fluid flow (such as the Navier-Stokes equations) under the assumption that the flow conditions do not vary with time. This allows for the determination of the equilibrium flow field, providing valuable insights into the performance and

behavior of the fluid system. Common applications of time-independent tests in CFD include the analysis of airflow around aerodynamic surfaces, the study of heat transfer in stationary systems, and the evaluation of fluid behavior within steady-state industrial processes. By conducting timeindependent tests in CFD, engineers and researchers can gain a better understanding of the fluid dynamics within various systems, enabling them to optimize designs, improve performance, and make informed engineering decisions. Above figure show the time independent test for our work after 10^{-4} s, our results have not changed.

According to time independent study ideal time step is 10^{-5} s which matched with the value of another time step $10^{-6}s$. As it can be seen at Pietersen's [40] study the solver of mhdFoam includes PISO loop which starts to solve momentum equation . Also, in Pietersen's work includes the value as 10^{-5}s for all parameters like U, B, B_t and B_{fixed} and also they have tend to give similar results for 10^{-6} as it can be seen in the graph above.

3.4 Validation

The current section of the thesis is dedicated to validating our results by comparing them with the results from the existing literature. To accomplish this, we used the dimensions from Pietersen's work [40], specifically the dimensions listed in the table he used to study the behaviors of the Orszag-Tang vortex with cyclic boundary conditions. The comparison results indicate a strong agreement with Pietersen's work.

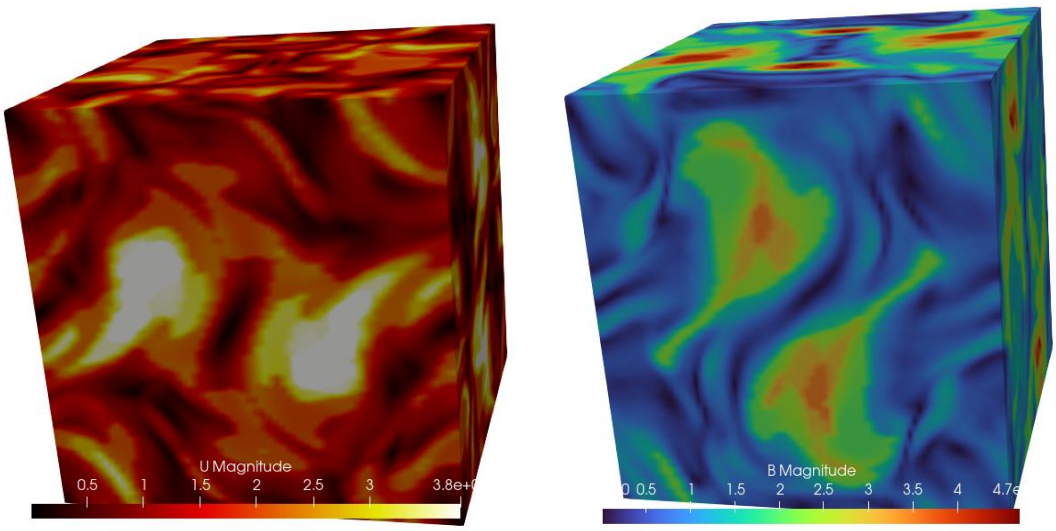

Figure 3.3 Comparison of present work and Pietersen's work [40]

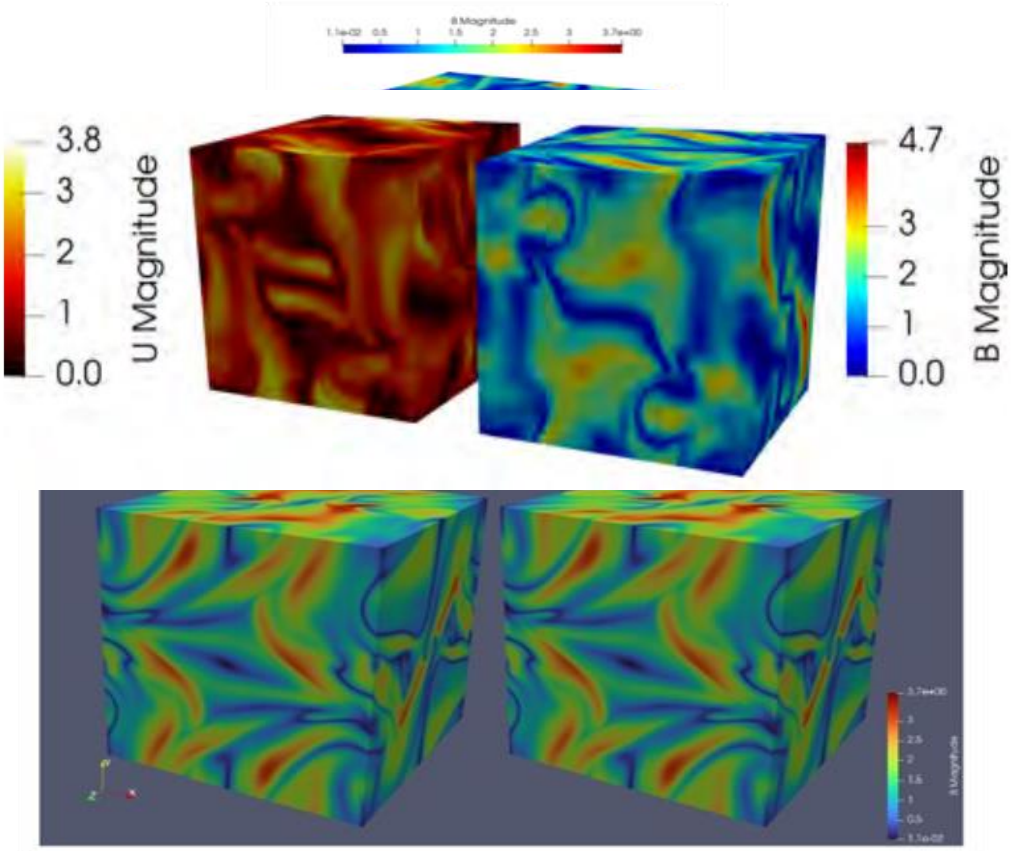

Figure 3.4 Gonzalez's work for U and B magnitudes

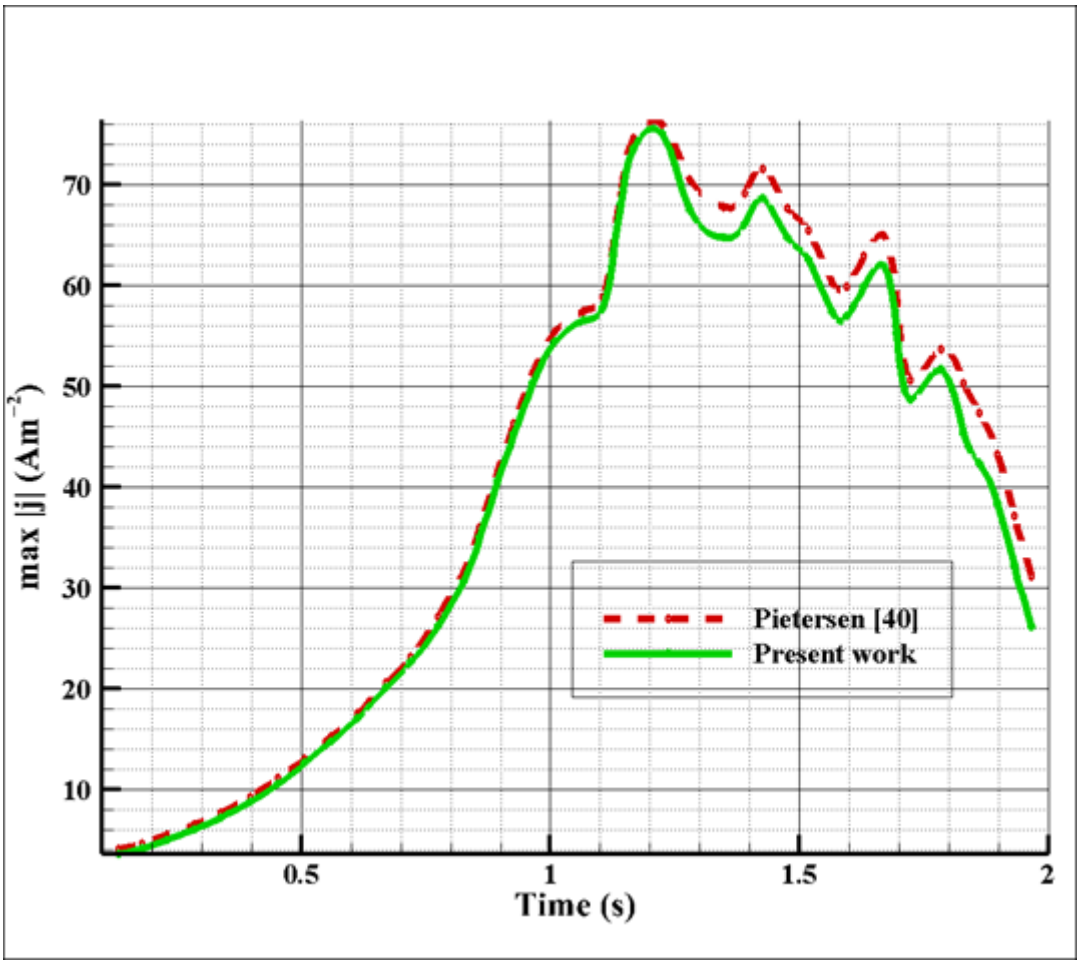

Figure 3.5 Present work for U and B magnitudes [49]

3.4.1 Mesh Independence Study

In computational fluid dynamics (CFD) simulations, it is important to ensure that the numerical methods used are accurate and reliable to obtain accurate results. Two important aspects of CFD simulations are mesh quality and time step size. The mesh quality is an important factor that affects the accuracy of CFD simulations. In CFD, a mesh is a discretization of the computational domain into small volumes or cells. The quality of the mesh can have a significant impact on the accuracy and convergence of the simulation results. A poorly designed mesh can lead to inaccurate results or numerical instability. To ensure the mesh quality, various metrics are used. One of the most used metrics is the aspect ratio, which is the ratio of the longest side

to the shortest side of a cell. A high aspect ratio indicates that the cell is highly distorted, which can lead to numerical instability. Other metrics used to assess the mesh quality include skewness, orthogonality, and smoothness. The time step size is another important factor in CFD simulations. The time step size determines the accuracy and stability of the simulation. A time step that is too large can lead to numerical instability, while a time step that is too small can result in a long simulation time.

To ensure the appropriate time step size, time step tests are performed. In a time, step test, the simulation is run at different time step sizes, and the results are compared to a reference solution or experimental data. The time step size is then selected based on the accuracy and stability of the simulation. In conclusion, the mesh quality and time step size are important factors that affect the accuracy and reliability of CFD simulations. To ensure accurate results, it is important to perform mesh quality and time step tests in CFD simulations. In present work, we selected three types of mesh to converge our results and independence of results from mesh.

Figure 3.8 shows the various configuration of shocks versus length of domain for various mesh sizes. According to this figure, we found that 8.10^6 meshes is optimum and suitable for our work. After this value of mesh size, the results have not any significant changes. These results showed that the time step of 10^{-4} is suitable for present numerical work. The selecting method of time step was like mesh independent test method. However, both Gonzalez [49] and Pietersen [40] took time step as 10^{-3}.

In the context of Computational Fluid Dynamics (CFD), a time independent test refers to a simulation or analysis in which the flow conditions and parameters are assumed to remain constant over time. This type of test is often used to evaluate the steady-state behavior of a fluid flow within a given system. In CFD, engineers and researchers often use time-independent simulations to study the flow patterns, pressure distributions, and other characteristics of a fluid within a specific geometry or environment. These simulations are particularly useful for understanding the behavior of fluid systems under steady-state conditions, where the flow variables do

not change with time. Time-independent tests in CFD involve solving the governing equations of fluid flow (such as the Navier-Stokes equations) under the assumption that the flow conditions do not vary with time. This allows for the determination of the equilibrium flow field, providing valuable insights into the performance and behavior of the fluid system. Common applications of time-independent tests in CFD include the analysis of airflow around aerodynamic surfaces, the study of heat transfer in stationary systems, and the evaluation of fluid behavior within steady-state industrial processes. By conducting time independent tests in CFD, engineers and researchers can gain a better understanding of the fluid dynamics within various systems, enabling them to optimize designs, improve performance, and make informed engineering decisions. Above figures show the time independent test for our work after 10^{-4} s, our results have not changed.

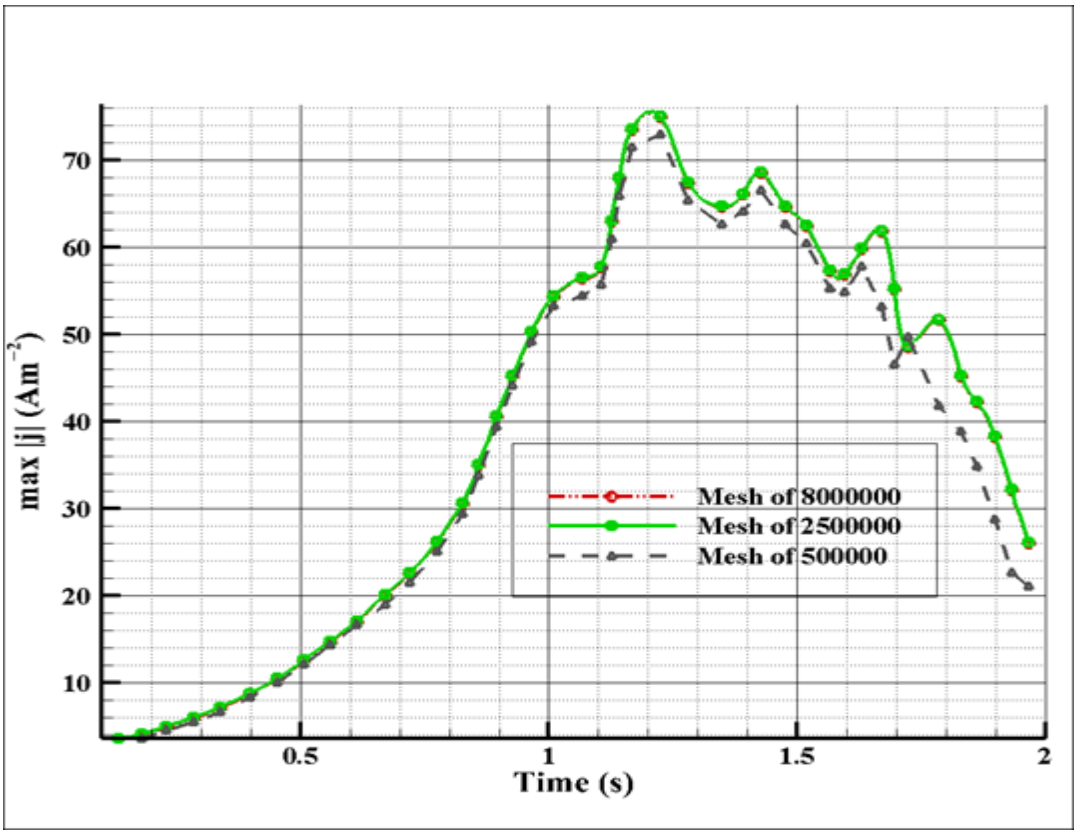

Figure 3.6 Mesh independent test

Table 3.3 Mesh Parameter

Mesh	$\Delta x = \Delta y = \Delta z$	Number of cells
I	$\frac{L}{(N-1)}$	N^3
II	$\frac{L}{(2N-1)}$	$(2N)^3$
III	$\frac{L}{(4N-1)}$	$(4N)^3$

3.5 Results

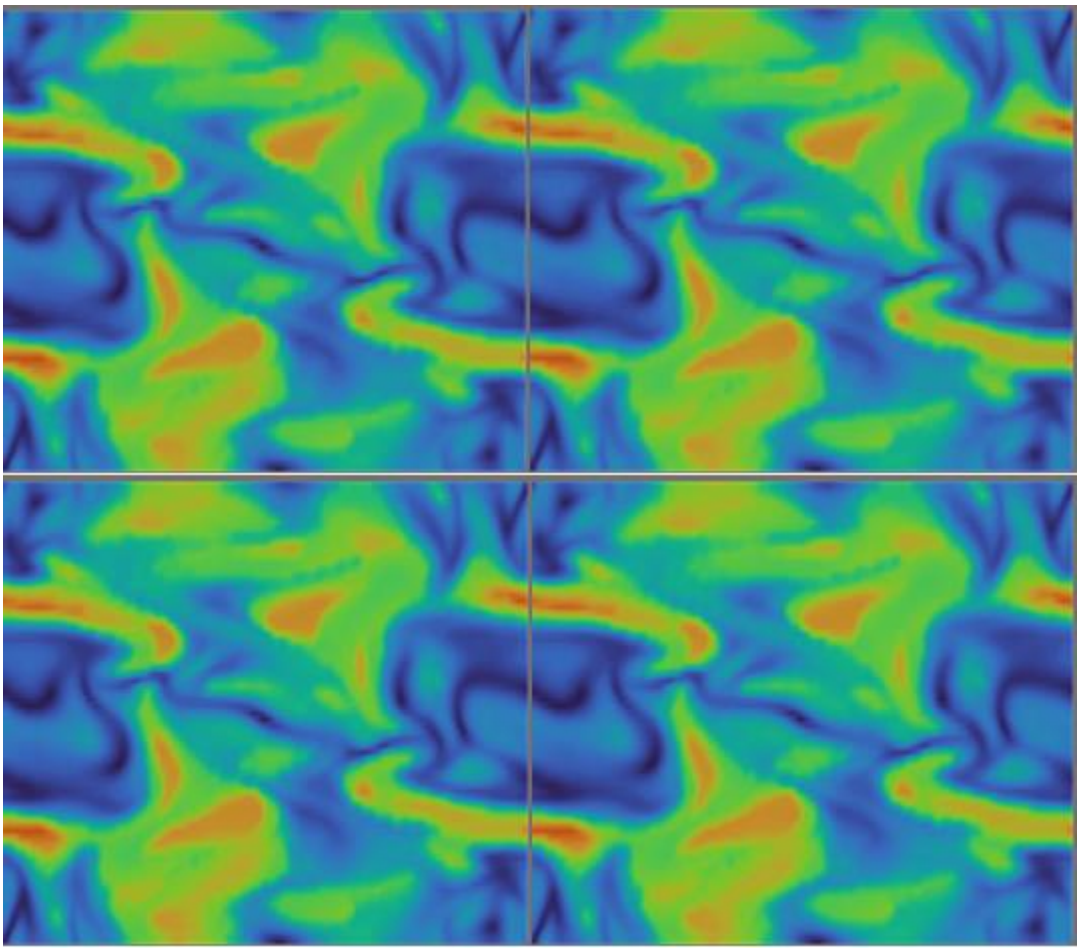

Figure 3.7 Centeral vortex slice of B magnitude

Orszag-Tang vortex visual taken as a slice at the center of simulation. Parawiev already has the propertiy tool which can be used easily. There is no need to enter exact points of slice position . It can be easily seen that magnetic vortex structures in two dimensional periodic domain.

The solution contributes a piece of scales and similar to turbulence behavior which makes it hard to observe but good benchmark problem to observe the accuracy and efficiency of codes developed for simulating fluid flows.

It is common to use the Orszag-Tang vortex as a classic test problem to understand the efficiecy of numerical models and to compare different simulation techniques in the field of fluid dynamics. It is convinient to develop new mathematical pathways and also to understand the behavior of turbulence and vortex interactions in fluid flows and supply a basement for validating and improving computational methods.

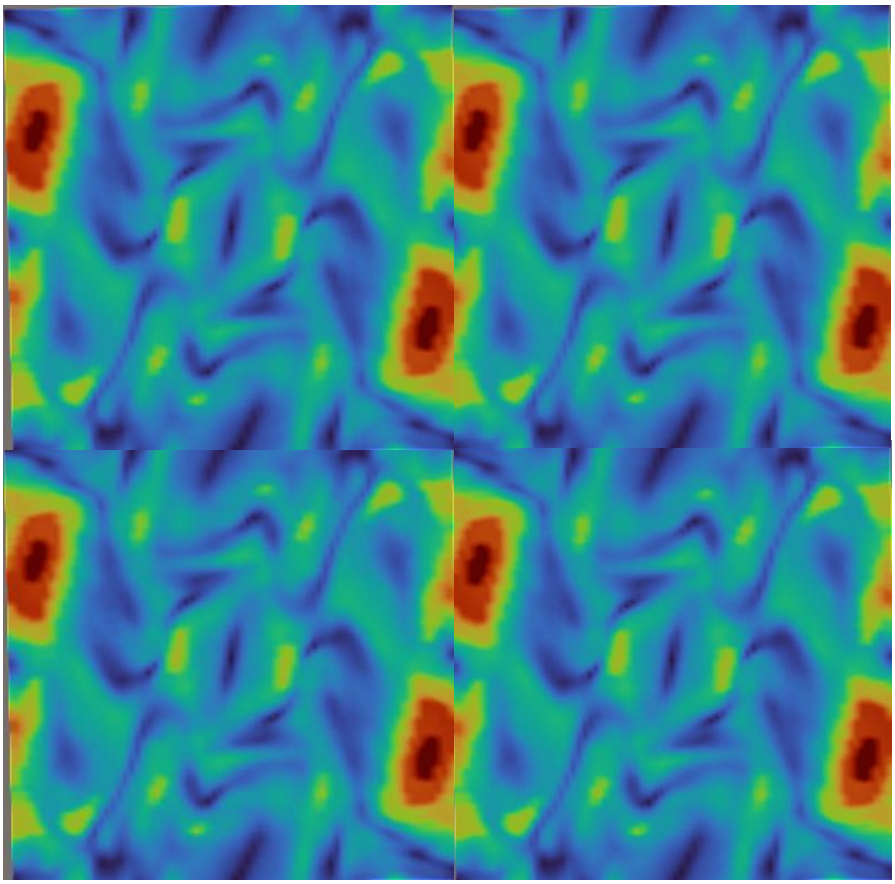

Figure 3.8 Central vortex slice of U magnitude

3.5.1 Effects of density on 3D Orszag-Tang vortex

The Orszag-Tang vortex is a fundamental fluid dynamics phenomenon that arises when two fluids of different densities and velocities interact. The behavior of the vortex is heavily influenced by the density of the fluids. In a three-dimensional Orszag-Tang vortex, altering the density of the fluids can significantly impact the behaviors of the vortex. As the fluid density increases, the vortices become more

stable and can persist for longer durations. This increased stability is attributed to the greater resistance of the denser fluids to vortex deformation. In contrast, a decrease in the fluid density causes the vortices to be less stable and dissipate more rapidly. This is because of the reduced resistance of the fluid to vortex deformation.

The impact of fluid density on the behaviors of the Orszag-Tang vortex has far-reaching implications for scientific and engineering fields. Understanding the behaviors of the vortex at different density regimes is vital for predicting fluid flow behaviors in natural and engineered systems like atmospheric and oceanic flows. Additionally, knowledge of the vortex's behaviors can be applied in the design of fluid-based technologies like pumps, turbines, and heat exchangers. In conclusion, the effects of fluid density on the attitude of the three-dimensional Orszag-Tang vortex are a crucial area of research with broad implications for fluid dynamics and its various applications.

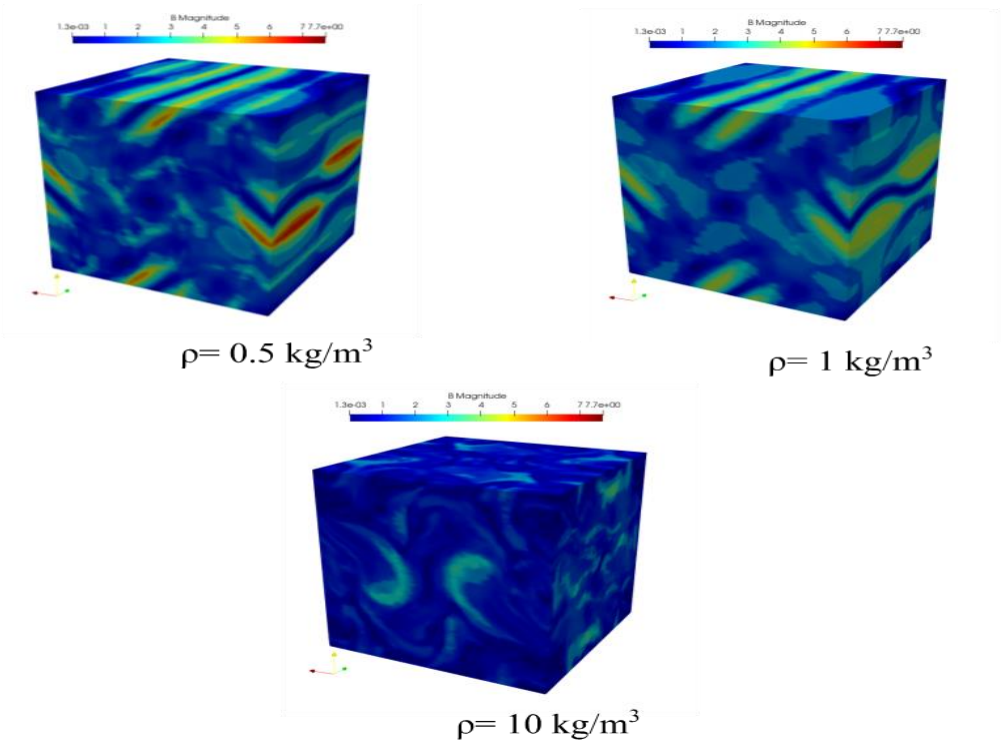

Figure 3.9 Effects of density on vortex

According to the study results and simulations indicates that; pressure based 3-D Orszag -Tang problem test case, flow has become turbulance while density of the fluid increased. Fluid dynamics and gas dynamics researches focuses on different effects of different parameters over flow. Also similar observation can be seen easily from the graph takes place ,in next part.

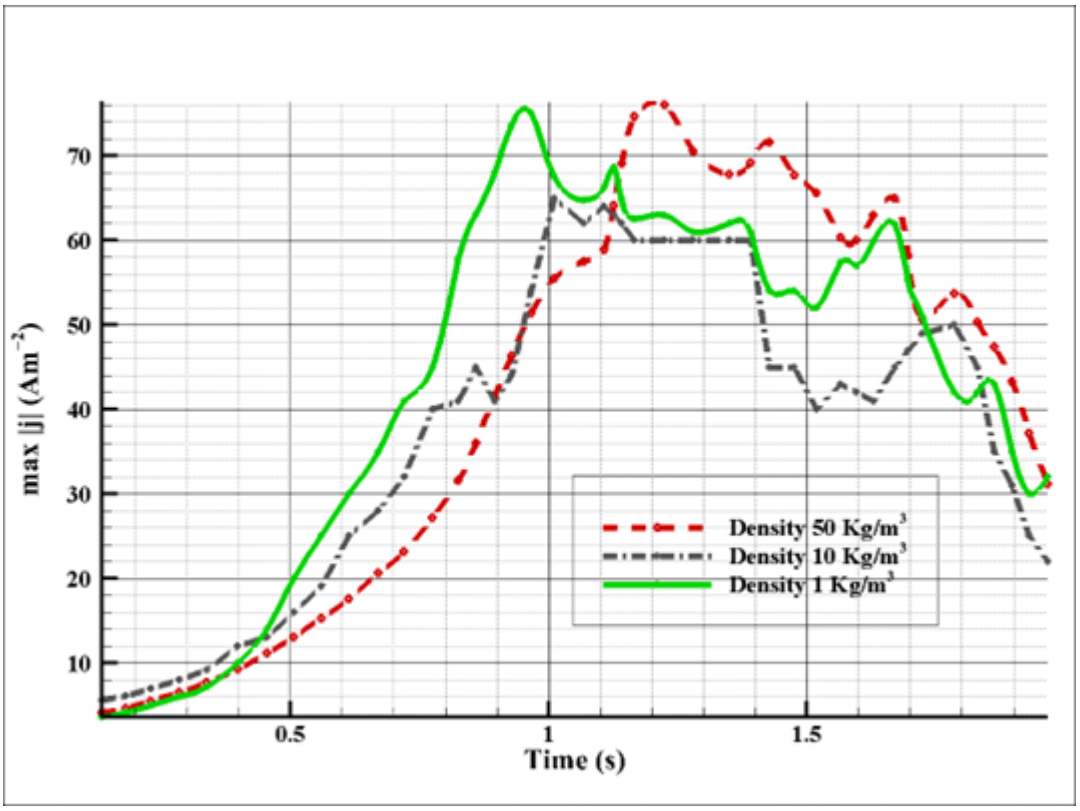

Figure 3.10 Variations of max current density over the time for various density

This graph shows up to time of 1s all fluids, has different density, tend to increase maximum current density. However, after then fluctiations has started also more denser fluid reaches the most high value of current density after the point. While until the point less denser fluid had the maximum current density level.

All these observations points out flow has started to become turbulent after the 1s time line. Ionized gas or super conductor which means ideal plasma can be easily manipulated by density factor which gaves the change of control fluid flow in a certain cases or applications.

3.5.2 Effects of Reynolds Number on 3D Orszag-Tang Vortex

The Reynolds number is a non-dimensional parameter that characterizes fluid flows, including the attitude of the Orszag-Tang vortex. The impact of Reynolds number on the three-dimensional Orszag-Tang vortex is of great interest to the fluid dynamics community. As Reynolds number rises, the performance of the Orszag-Tang vortex undergoes significant changes. Lower Reynolds numbers result in regular, organized vortex structures. However, as Reynolds number increases, the vortex becomes increasingly complex and chaotic, with the emergence of smaller secondary vortices. The effects of Reynolds number on the dynamics of the Orszag-Tang vortex are especially evident near the vortex core. At lower Reynolds numbers, the vortex core exhibits a smooth, stable structure. Conversely, at higher Reynolds numbers, the vortex core becomes more turbulent and disordered, with smaller eddies forming.

These effects of Reynolds number on the behaviors of the Orszag-Tang vortex have important implications across a range of scientific and engineering fields. For example, understanding the behaviors of the vortex at different Reynolds numbers is crucial for predicting the fluid dynamics of various natural and engineered systems, such as atmospheric and oceanic flows. Additionally, this knowledge is useful in designing fluid-based technologies, such as heat exchangers, pumps, and turbines. In conclusion, the effects of Reynolds number on the behaviors of the three-dimensional Orszag- Tang vortex are an essential research area with broad implications for fluid dynamics research and applications.

The Reynolds number has an important characteristic in the domain of ideal plasma, which is a parameter to determine the properties of the Orszag-Tang vortex. The parameter affects its transition to turbulence, vortex structure, and all bahaviour.. Although, it is often discover a range of Reynolds numbers to contribute insights into

the gas dynamics and turbulence of fluid flows using the Orszag-Tang vortex as a benchmark test problem.

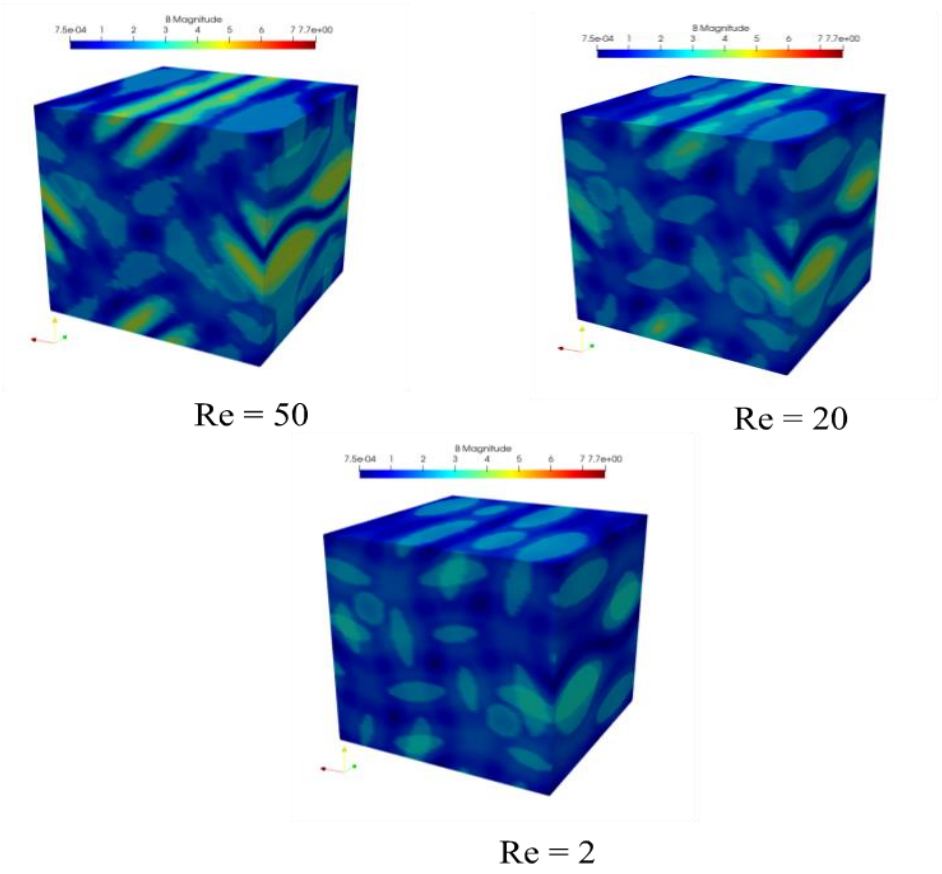

Figure 3.11 Effects of Reynolds number on the vortex

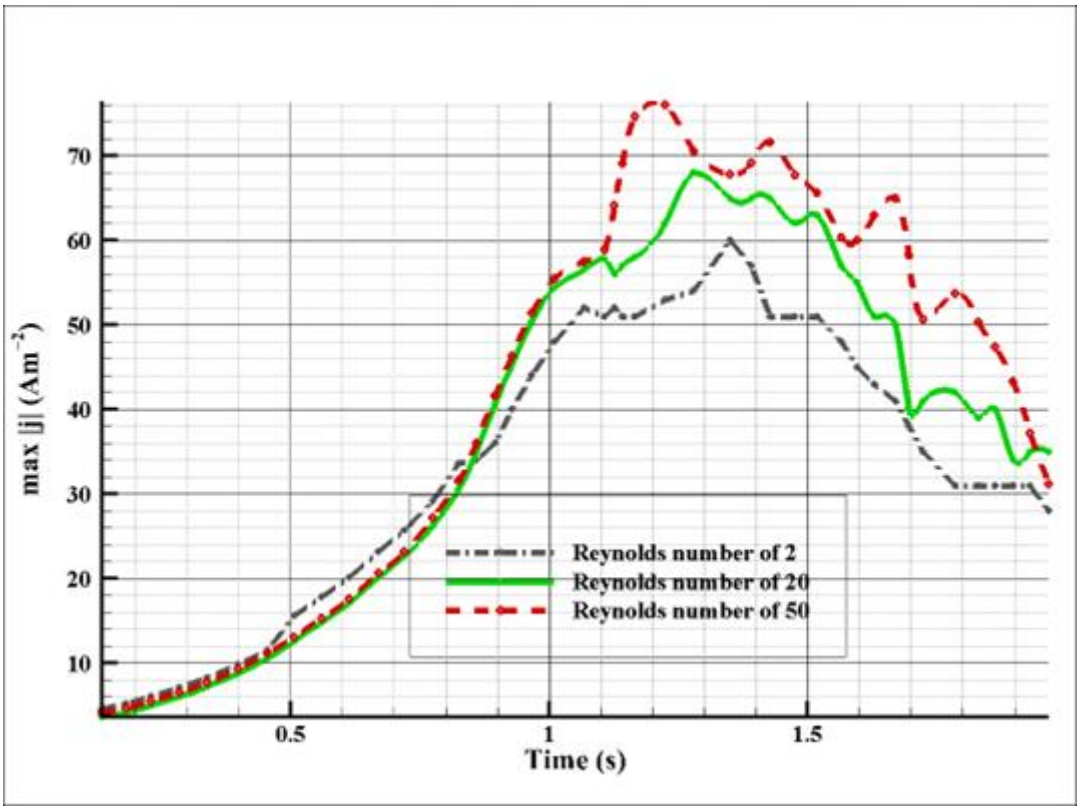

Figure 3.12 Variations of max current density over the time for various Reynolds numbers

3.6 Effects of Magnetic Field on 3D Orszag-Tang Vortex

The Orszag-Tang vortex is a fundamental phenomenon in fluid dynamics that emerges when two fluids of different densities and velocities interact. The attitude of this vortex is also influenced by the presence of a magnetic area, which has a significant impact on its performance. As the magnetic area strength increases, the behaviors of the three-dimensional Orszag-Tang vortex undergoes significant changes. At lower magnetic area strengths, the vortex exhibits characteristics like those observed in its absence. However, as the magnetic area strength increases, smaller vortices form within the main vortex, making its behaviors more complex. The effects of the magnetic area strength on the behaviors of the Orszag-Tang vortex are most evident near the vortex core.

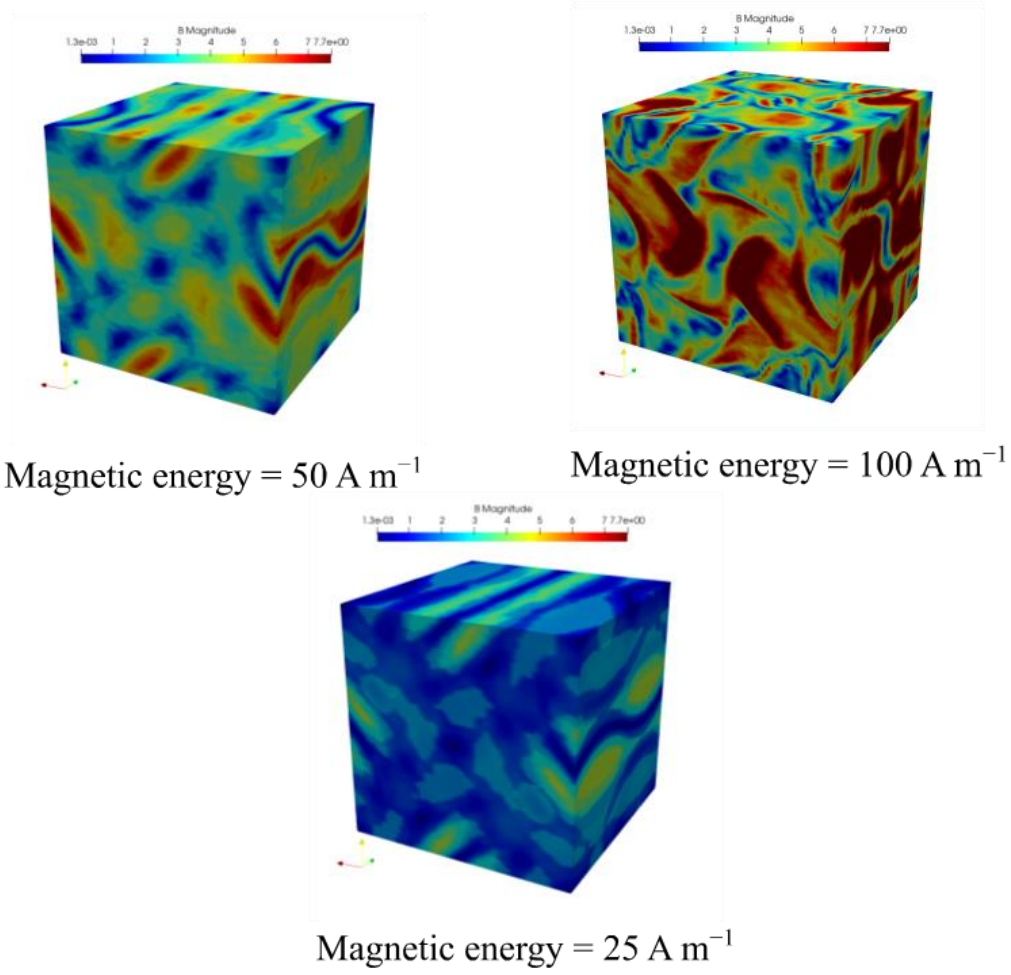

Figure 3.13 Effects of magnetic field on the vortex

At lower magnetic area strengths, the core is relatively stable and has a well- defined structure. However, at higher magnetic area strengths, the core becomes more turbulent and disordered, with the formation of smaller eddies. The effects of magnetic area strength on the performance of the Orszag- Tang vortex have significant implications for scientific and engineering fields. Understanding the behaviors of the vortex at different magnetic field strengths is vital for predicting fluid flow behaviors in various natural and engineered systems, such as atmospheric and oceanic flows.

Additionally, knowledge of the vortex's behaviors under the influence of a magnetic area is critical for designing magnetic fluid-based technologies like magnetic pumps and magnetic drug delivery systems. To summarize, the effects of magnetic area

strength on the performance of the three-dimensional Orszag-Tang vortex is a crucial area of study with broad implications for fluid dynamics research and its various applications.

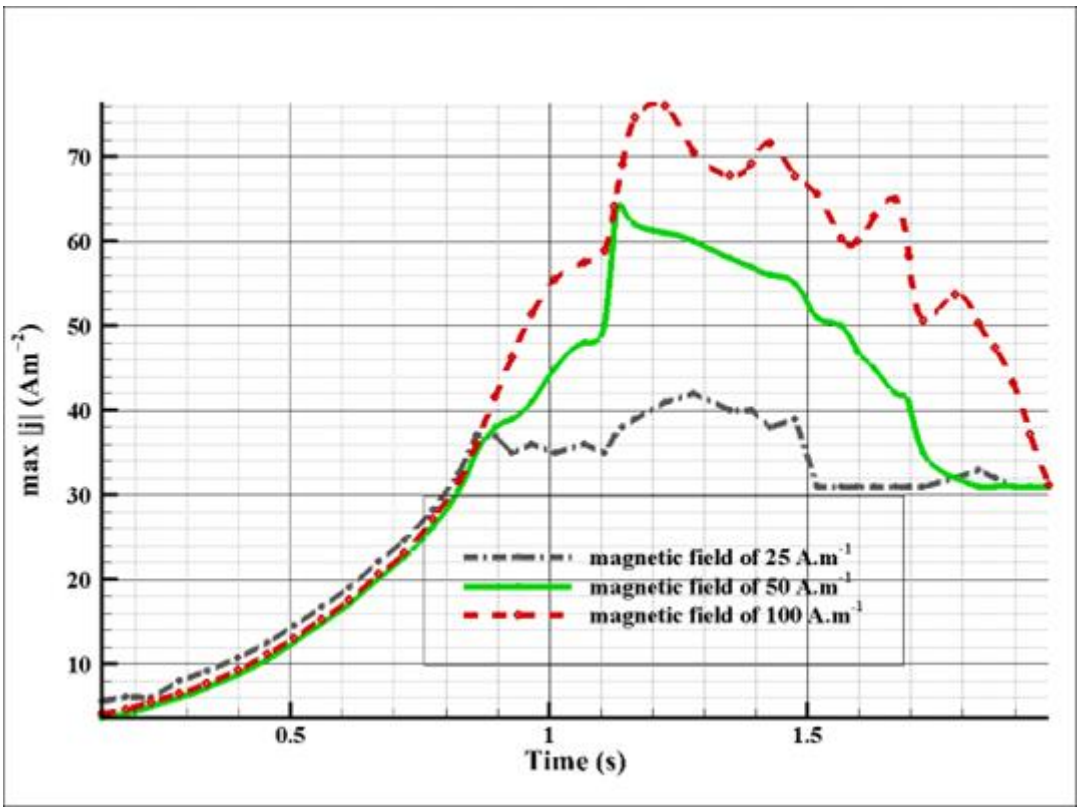

Figure 3.14 Variations of max current density over the time for various magnetic fields

The graph indicates that after point 0.8 s with under effect of different magnetic fields start to make difference in its behaviour with respect to the raising current density. The more system has been effected from magnetic field the more current density increases.

3.7 Effects of Hartmann Number on 3D Orszag-Tang Vortex

The Hartmann number is a dimensionless parameter that quantifies the magnetic area strength in a conducting fluid. The presence of a magnetic area has a significant impact on the dynamics of the three-dimensional Orszag-Tang vortex, and the

Hartmann number plays a pivotal role in determining the vortex's actions. As the Hartmann number increases, the attitude of the Orszag-Tang vortex undergoes significant changes. At lower Hartmann numbers, the vortex behaves similarly to the absence of a magnetic area. However, as the Hartmann number increases, the vortex becomes more intricate and turbulent, with the emergence of smaller vortices.

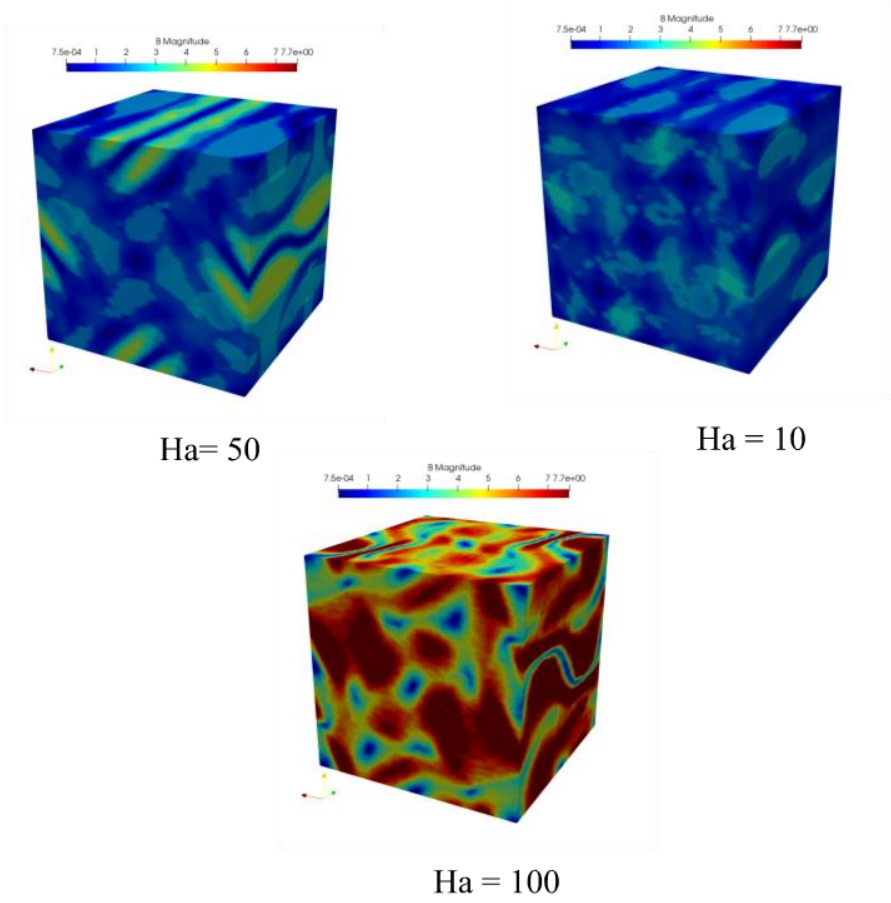

Figure 3.15 Effects of Hartmann number on the Orszag-Tang vortex

The effects of the Hartmann number on the behaviors of the Orszag-Tang vortex are most pronounced near the vortex core. At lower Hartmann numbers, the core is relatively stable, with a smooth and well-defined structure. However, at higher Hartmann numbers, the core becomes more turbulent and disordered, with the formation of smaller eddies and secondary vortices.

The Hartmann number's effects on the Orszag-Tang vortex performance have significant implications for scientific and engineering areas. Understanding the vortex's behaviors at various Hartmann numbers is crucial for predicting fluid flow performance in natural and engineered systems, such as atmospheric and oceanic flows.

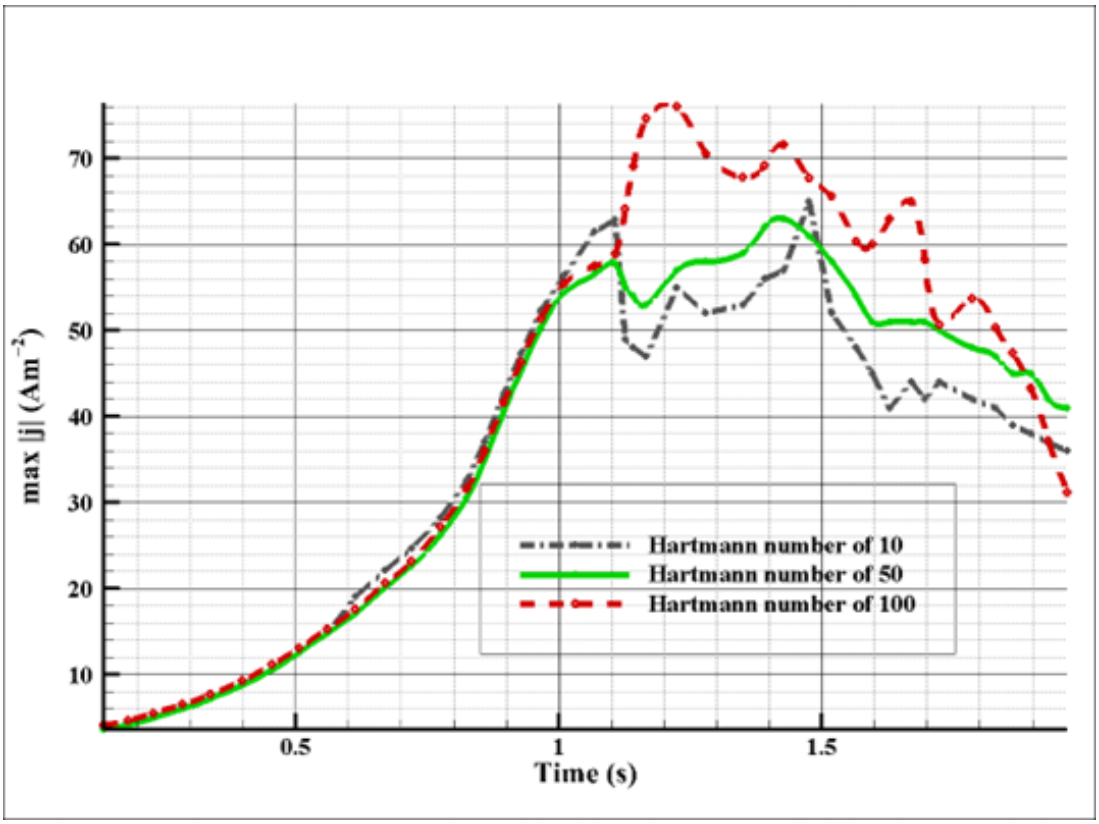

Figure 3.16 Variations of max current density over the time for various Hartmann number

The Hartmann number's effects on the Orszag-Tang vortex performance have significant implications for scientific and engineering areas. Understanding the vortex's behaviors at various Hartmann numbers is crucial for predicting fluid flow performance in natural and engineered systems, such as atmospheric and oceanic flows.

Furthermore, information about the vortex's behaviour under a magnetic area is essential for developing magnetic fluid- based technologies, such as magnetic pumps

and drug delivery systems. In conclusion, the Hartmann number's effect on the behaviour of the three-dimensional Orszag-Tang vortex is a vital research area with broad implications for fluid dynamics research and its various applications

CHAPTER 4

COMPUTATIONAL TEST CASE SHOCK-CLOUD

4.1 INTRODUCTION

The sock-cloud interaction case refers to the phenomenon that occurs when a shock wave interacts with a cloud or aerosol particles suspended in the air.

When a shock wave passes through a cloud, it can cause complex interactions and dynamic changes within the cloud structure. These interactions can result in the formation of new cloud droplets, changes in droplet size distribution, and alterations in cloud properties such as cloud reflectivity and lifetime. The sock- cloud interaction case is of particular interest in atmospheric science and cloud physics, as it plays a role in understanding cloud formation, cloud-air interactions, and their impact on weather and climate.

The shock-cloud interaction case involves the study of the interaction between shock waves and clouds or aerosol particles in the atmosphere. When a shock wave passes through a cloud, it compresses and heats the air, leading to dynamic changes within the cloud. One key aspect of this interaction is the formation of new cloud droplets. The compression of the air by the shock wave can cause supersaturation, where the air becomes saturated with water vapor, leading to the nucleation and growth of new cloud droplets. This process can contribute to cloud development and potentially affect cloud properties such as cloud cover, cloud height, and cloud lifetime.

4.2 PROBLEM DESCRIPTION

The shock-cloud interaction can lead to changes in the size distribution of cloud droplets. The shock wave can cause droplet coalescence or fragmentation, altering

the droplet size distribution within the cloud. These changes can have implications for cloud optical properties, such as cloud reflectivity and scattering of sunlight, which in turn can influence the radiative balance of the atmosphere.Understanding the sock-cloud interaction case is important for various applications. In weather forecasting, it can help improve predictions of cloud formation and cloud evolution in response to atmospheric disturbances. In climate studies, it can contribute to a better understanding of aerosol-cloud interactions and their impact on the Earth's energy balance. Researchers use numerical models, laboratory experiments, and field observations to investigate the sock-cloud interaction case. These studies aim to unravel the complex mechanisms involved and provide insights into the dynamic processes occurring within clouds when subjected to shock waves.

The shock-cloud interaction case involves modelling the interaction between a denser supersonic cloud and a strong shockwave. In this study, an imposed transverse magnetic field is also considered, leading to the disruption of the cloud. The computational domain is a square with coordinate values ranging from 0 to 1 in the x and z directions. The shockwave is positioned at x = 0.05, while the center of the denser cloud is located at (0.25, 0, 0.5), with a cloud radius of 0.15. The initial conditions for the left and right states of the shock location are specified.

4.2.1 Problem statement

In addition, the density and pressure within the cloud's radius are specified as 10 and 1, respectively. The simulation is carried out until a time of t = 0.06, and the obtained results are compared with the findings of Yalim [42] and Toth [43]. The density contours depicted in Figure 4..1 shows the disruption of the cloud, along with various features such as the detached bow shock ahead of the cloud, compression of the upstream front of the cloud, elongation of the cloud in the downstream direction, and a recompression shock at the tail of the cloud, among other complex flow features.

The plot of magnetic field lines shown in Figure 4.2. demonstrates that the transverse magnetic field has penetrated the cloud, creating a highly intricate pattern. These

flow and magnetic area patterns exhibit good agreement with the results reported in the before mentioned references. This simulation highlights the robustness and accuracy of the current code in predicting complex magnetohydrodynamic (MHD) flows. In daily life example Wilson cloud is a case.

The shock cloud becomes visible during daily life named as Wilson clouds. These type of clouds are not shock waves by own but they take places behind it. As soon as weather have a sudden drop where air pressure through high to low, the capacity of the air to contain water vapor lowered as well. The condensed water vapor comes out of the air and results in a visible cloud. This cloud rapidly distincts as soon as once the low pressure region behind the shockwave goes on and the local pressure comes to normal. At these point the instant shock and cloud interaction case results in air drops seperation in to various number of small pieces.

4.2.2 Mesh and tıme ındependent test for shock cloud ınteractıon

In this section of the thesis, our focus was on conducting time and mesh independent tests for a specific electromagnetic application, namely shock cloud interactions. Our findings revealed that a mesh count of 500,000 is suitable, with minimal variation compared to a mesh count of 1,000,000. To assess this, we examined three mesh configurations: 200,000, 500,000, 1,000,000, and 2,000,000. In terms of time step independence, we determined that a time step of 10^{-4}s is appropriate for our work.

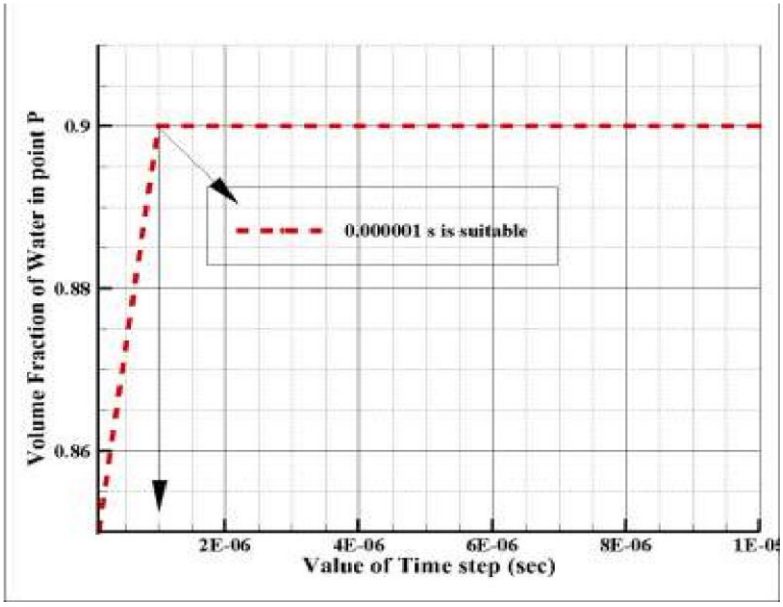

P

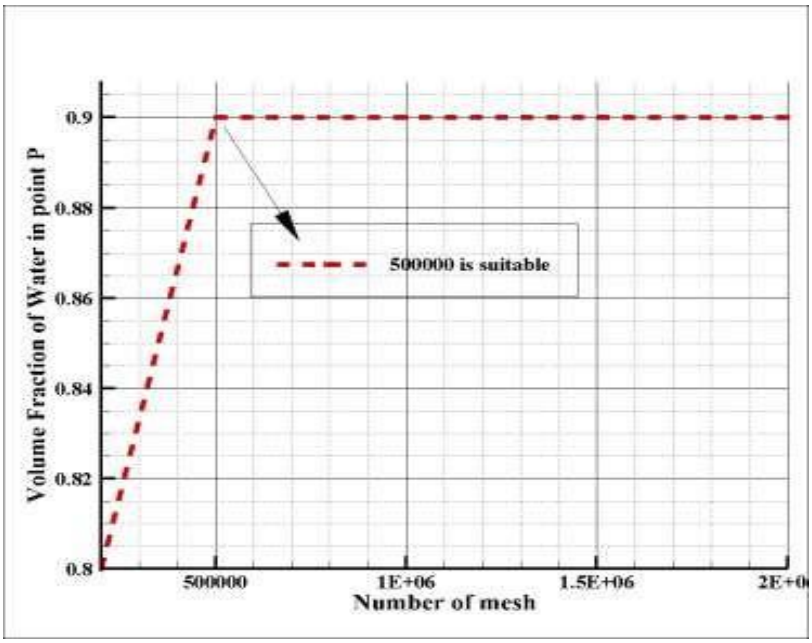

Figure 4.1. Time and mesh independent test for shock cloud interactions

4.2.3 Q criteria

The Q criteria is a technique utilized in fluid mechanics to detect vortices in fluid flow by determining their strength and location. Vortices refer to regions of swirling flow characterized by the rotation of fluid particles around an axis, and they are prevalent in various fluid flow applications, including aerodynamics, oceanography, and industrial processes. The Q criteria involves analyzing the second invariant of the velocity gradient tensor to identify vortices mathematically. This mathematical method operates on the premise that vortices have high values of the second invariant, whereas non-vortex regions have low values of the second invariant. The Q criteria can be expressed mathematically as:

$$Q = \lambda_2 - \lambda_3 - \lambda 3 \quad (4.1)$$

The Q criteria is a scalar field that is calculated using the second and third eigenvalues of the velocity gradient tensor (λ_2, λ_3 , respectively) and provides a quantitative measure of the strength and location of vortices in the fluid flow field. This method is useful for visualizing and analyzing vortex behaviour in fluid flow, and it can be used to identify the location and strength of vortices over time. This information is valuable for understanding fluid flow behaviour and designing fluid flow schemes for specific applications. In this study, the Q criteria was applied to calculate the presence of vortices in an electromagnetic sock and cylindrical fluid. When the Q criteria value is high, it indicates that vortices are capturing the uniform flow and reducing the increasing instabilities. Vortex flow can also increase the separated flow over the leading edge and increase drag forces. vortex Q criteria behaviour during the interaction with cylinder fluid and electromagnetic shock have been shown in Figure 4.1

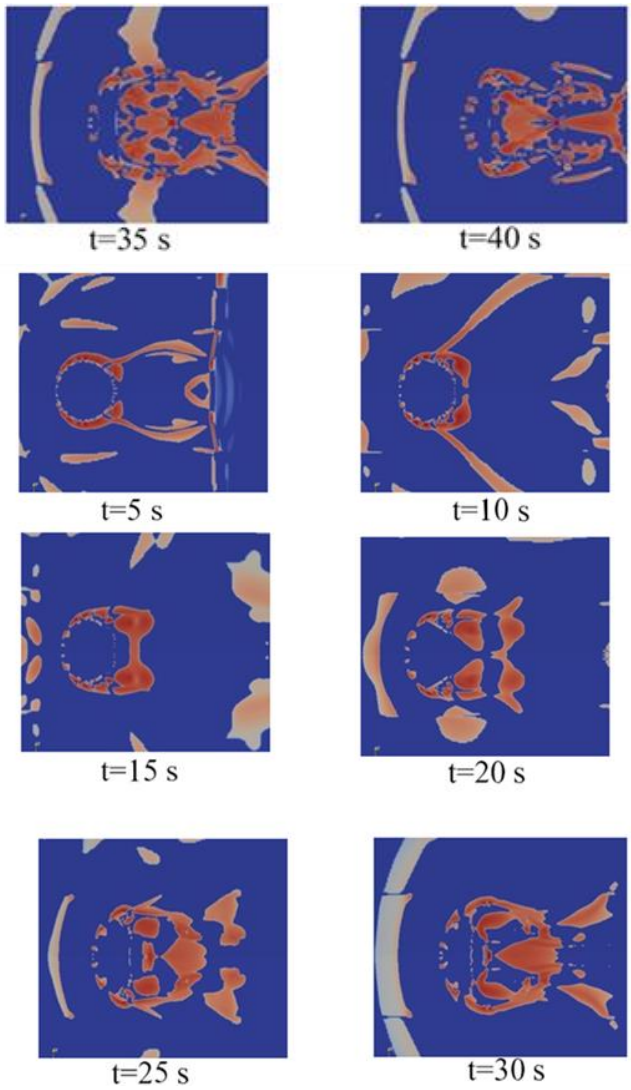

Figure 4.2. Vortex Q criteria behaviour during the interaction with cylinder fluid and electromagnetic shock

4.3 RESULTS

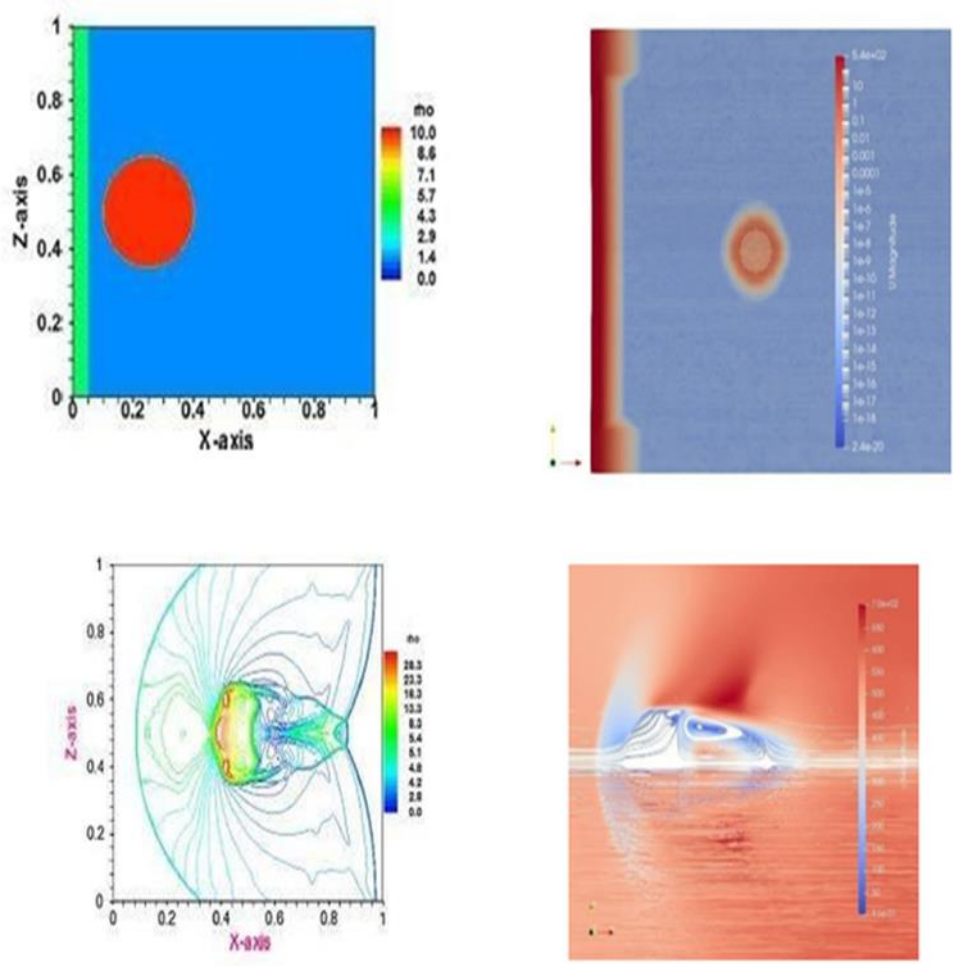

Figure 4.3. Comparison between present work and Balasubramanian[4].

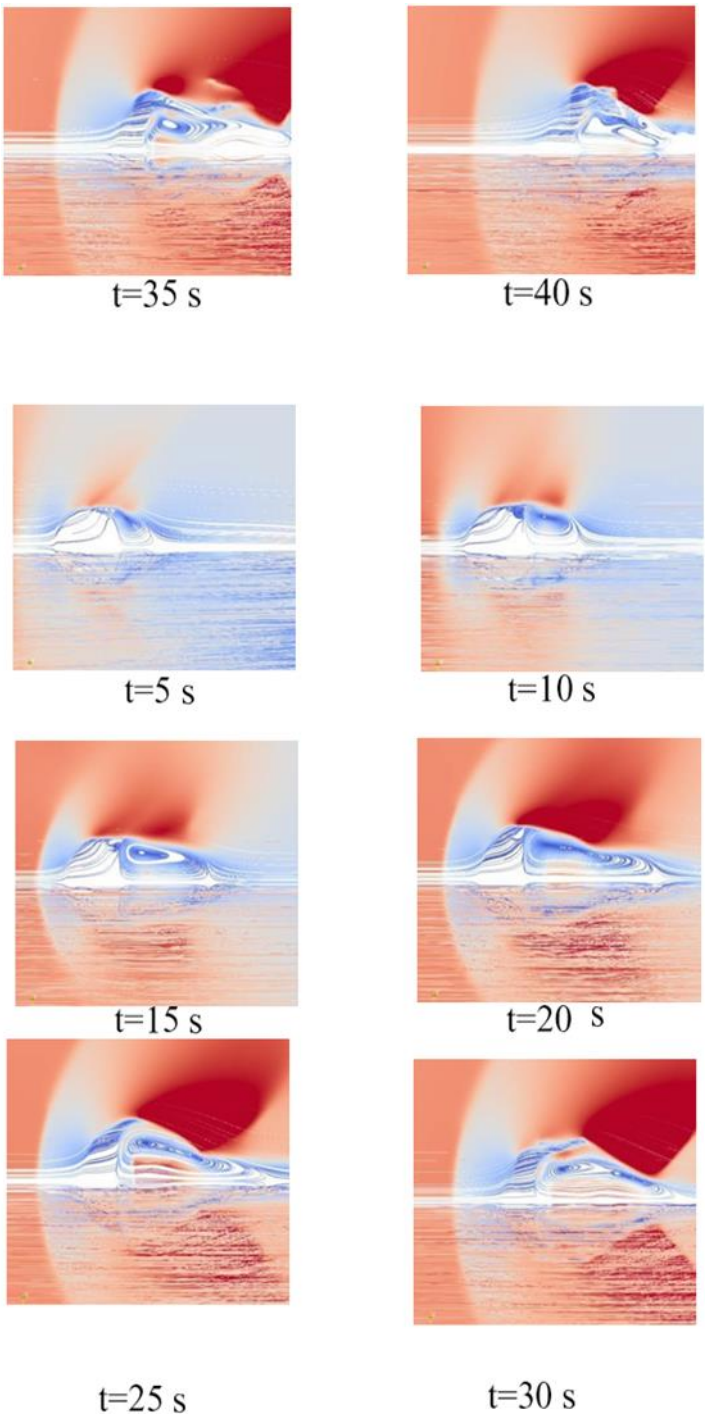

Figure 4.4. Electromagnetic shock behaviour during the interaction with cylinder fluid

4.3.1 Volume of Fluid Method

Vortex-Induced Vibration is a phenomenon that occurs when a fluid flow interacts with a cylindrical structure, leading to the formation of vortices and subsequent vibrations. When coupled with electromagnetic shocks, this interaction becomes even more complex and fascinating. When a fluid flows past a cylinder, it creates alternating vortices on the opposite sides of the cylinder. These vortices generate a periodic shedding pattern, commonly known as Karman Vortex Street. As these vortices are shed, they induce forces on the cylinder, causing it to vibrate. This vibration is known as Vortex-Induced Vibration. Now, when an electromagnetic shock is introduced into this system, it adds another layer of complexity to the interaction. An electromagnetic shock is a sudden and intense release of electromagnetic energy. When this shock interacts with the fluid flow and the vibrating cylinder, various interesting phenomena can occur.Firstly, electromagnetic shock can influence the shedding pattern of the vortices. It can disrupt the regular formation of Karman Vortex Street, leading to an irregular and chaotic shedding of vortices. This can significantly affect the vibration characteristics of the cylinder, causing it to exhibit unpredictable motion. Secondly, the electromagnetic shock can induce additional forces on the cylinder. These forces can be attractive or repulsive, depending on the nature of the shock and the properties of the cylinder. These additional forces can either amplify or dampen the existing vibrations, leading to changes in the overall behaviour of the system.

Furthermore, the electromagnetic shock can also alter the fluid flow around the cylinder. It can create disturbances in the boundary layer, leading to changes in the flow velocity and pressure distribution. These changes can further affect the vortex shedding and, consequently, the vibration characteristics of the cylinder.

Overall, the interaction between VoF behaviour, cylinder fluid, and electromagnetic shocks is a complex and dynamic phenomenon. It involves the interplay of fluid dynamics, structural mechanics, and electromagnetic effects. Understanding and

predicting the behaviour of such schemes requires advanced computational models, experimental studies, and theoretical analyses.

Studying this interaction is of great importance in various engineering areas. It helps in designing structures that can withstand fluid-induced vibrations, such as offshore platforms, bridges, and tall buildings. Additionally, it aids in optimizing the achievement of systems that utilize fluid flow, such as heat exchangers,turbines, and aerospace vehicles. In conclusion, the interaction between VoF behaviour, cylinder fluid, and electromagnetic shocks is a fascinating and challenging area of research. It involves the study of fluid dynamics, structural mechanics, and electromagnetic effects to understand and predict the behaviour of such systems.

By gaining a deeper understanding of this interaction, engineers can develop more efficient and reliable structures and schemes. VoF behaviour during the interaction with cylinder fluid and electromagnetic shock have been showed in Figure 4.3.1

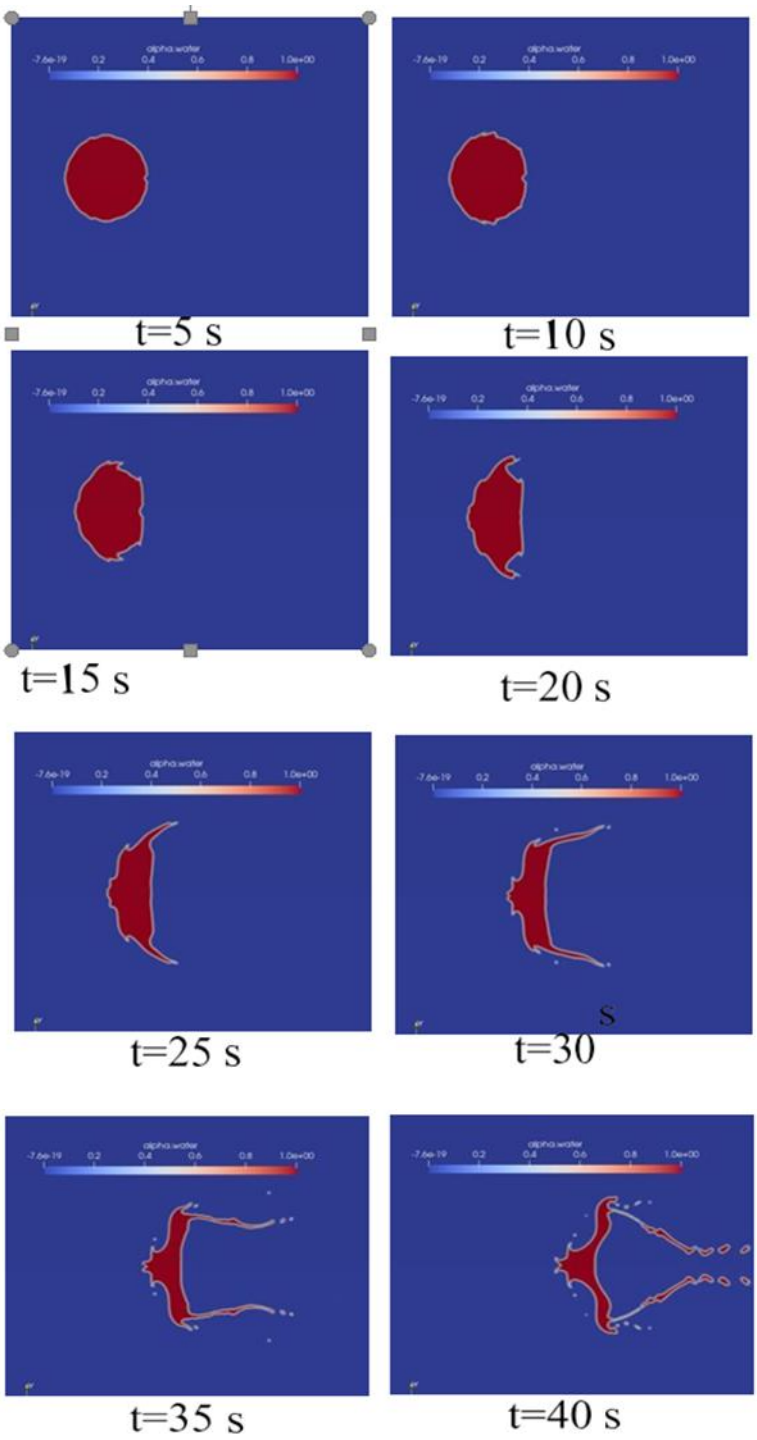

Figure 4.5. Vortex Q criteria behaviour during the interaction with cylinder fluid and electromagnetic shock

CHAPTER 5

CONCLUSION&FUTURE WORK

At the present comparative study, open-source code solvers, mhdFoam and multiphase solver compressible interFoam- elctromagneticsolver, are modified and combined to solve these problems. Solvers designed according to C++ program. Orszag-Tang is the main task of the thesis and two-phase shock-cloud interaction problem simulation made as MHD application. Shock-cloud interaction problem made in 2-D in many literatures work while Orszag-Tang vortex problem studied many dimensions. As a result of shock-cloud interaction case there are no charts on paper, instead they compare magnetic shock separation over visuals or streamlines. In the work, both these benchmark problems results matched with literature can be observed from charts takes place in results part of the work. Observation of the effect of different Re number, Ha number, magnetic area energy, density values overflow observed and compared with other sources. Furthermore, the time independence test gave the best results in the time10^{-5}s. It is also possible to do the same task with hybrid equations combination of Navier- Stokes and Maxwell equations mentioned by Tao, W. [44]. As a future work and as a target it is planned to developed new solver in OpenFoam that solves these benchmark cases it includes solenoidal constraint or design new OpenFOAM solver. The lack of Gauss Law constraint can cause many troubles in MHD area because it provides divergence cleaning. In future task divergence free constraint named as Powell's eight wave method will be used as divergence cleaning method [41]. Also, the same upwind method will be used as AUSM-PW+ and the same turbulence model will be used as RAS, k-Epsilon turbulence model. The newly developed solver will be intended to target plasma benchmark cases aims to solve some gas dynamics cases. The first task will be the Hypersonic Blunt Body case which aimsto flow control by using magnetic shock waves detection which as implementations in hypersonic flow. This time comparison of results will be done with literature work non-MHD solutions

REFERENCES

[1]Hosking, R. J., & Dewar, R. L. (2016). Fundamental fluid mechanics and magnetohydrodynamics. New York: Springer.

[2] Reyaz, R., Lim, Y. J., Mohamad, A. Q., Saqib, M., & Shafie, S. (2021). Caputo fractional MHD Casson fluid flows over an oscillating plate with thermal radiation. Journal of Advanced Research in Fluid Mechanics and Thermal Sciences, 85(2), 145-158.

[3] Waini, I., Ishak, A., & Pop, I. (2021). MHD Glauert flow of a hybrid nanofluid with heat transfer. Journal of Advanced Research in Fluid Mechanics and Thermal Sciences, 86(2), 91-100.

[4]Nayan, A., Fauzan, N. I. F. A., Ilias, M. R., Zakaria, S. F., & Aznam, N. H.

Z. (2022). Aligned Magnetohydrodynamics (MHD) Flow of Hybrid Nanofluid Over a Vertical Plate Through Porous Medium. Journal of Advanced Research in Fluid Mechanics and Thermal Sciences, 92(1), 51- 64.

[5] Körpınar, T., Demirkol, R. C., & Körpınar, Z. (2021). Optical magnetic helicity with binormal electromagnetic vortex filament flows in MHD.Optik, 247, 167544.

[6]Avdeeva, E. N., & Lukin, V. V. (2019, November). Divergence-free finite-difference method for 2D ideal MHD. In Journal of Physics: Conference Series (Vol. 1336, No. 1, p. 012026). IOP Publishing.

[7]Wang, X., Dai, Z., & Shen, Z. (2022). A 2D cell-centered Lagrangian scheme based on multi-state Riemann solver with exactly divergence-free magnetic fields. Journal of Computational Physics, 467, 111451.

[8] Cuissa, J. C., & Steiner, O. (2022). Innovative and automated method for vortex identification.

[9]Wang, X., Liu, S., Ban, X., Xu, Y., Zhou, J., & Kosinka, J. (2020). Robust turbulence simulation for particle-based fluids using the Rankine vortex model. The Visual Computer, 36, 2285-2298.

[10]Shuai, S., & Kasbaoui, M. H. (2022). Accelerated decay of a Lamb–Oseen vortex tube laden with inertial particles in Eulerian–Lagrangian simulations.

Journal of Fluid Mechanics, 936, A8.

[11]García, C. (2020). Kármán vortex street in incompressible fluid models. Nonlinearity, 33(4), 1625.

[12]Bayindir, C., & Akdemir, H. (2022, July). Prediction of the Spatiotemporal Dynamics of von Kármán Vortices by ANFIS. In Intelligent and Fuzzy Systems: Digital Acceleration and The New Normal-Proceedings of the INFUS 2022 Conference, Volume 1 (pp. 761-768). Cham: Springer International Publishing.

[13]Pastrana, D., Rodriguez, I., Cajas, J. C., Lehmkuhl, O., & Houzeaux, G. (2020). On the formation of Taylor-Görtler structures in the vortex induced vibration phenomenon. International Journal of Heat and Fluid Flow, 83, 108573.

[14] Hiejima, T. (2020). How the circulation and axial velocity deficit in Batchelor vortices affect their disturbance growth. Physics of Fluids, 32(7), 076107.

[15] Marusic, I., & Broomhall, S. (2021). Leonardo da Vinci and fluid mechanics. Annual Review of Fluid Mechanics, 53, 1-25.

[16] Ebrahimi, N. D., Eldredge, J. D., & Ju, Y. S. (2019). Wake vortex regimes of a pitching cantilever plate in quiescent air and their correlation with meanflow generation. Journal of Fluids and Structures, 84, 408-420.

[17] Karami, M., Carassale, L., & Hangan, H. (2020). Statistical and modal analysis of surface pressure fluctuations in tornado-like vortices. Physics of Fluids, 32(7), 075109.

[18] Berloff, P., Ryzhov, E., & Shevchenko, I. (2021). On dynamically unresolved oceanic mesoscale motions. Journal of Fluid Mechanics, 920, A41.

[19] Komitor, A. W. (2023). Comparing Finite Volume and Discontinuous Galerkin Methods for Magnetohydrodynamic Flows (Doctoral dissertation, University of Colorado at Boulder).

[20]Li, Y., Yang, S., Feng, F., & Tagawa, K. (2023). A review on numerical simulation based on CFD technology of aerodynamic characteristics of straight-bladed vertical axis wind turbines. Energy Reports, 9, 4360-4379.

[21] Hou, Y., Jin, K., Feng, Y., & Zheng, X. (2023). High-order targeted essentially non-oscillatory scheme for two-fluid plasma model. Applied

Mathematics and Mechanics, 44(6), 941-960.

[22] Han, S.H., Lee, J.I., Kim, K. H. (2009) Accurate and Robust Pressure Weight Advection Upstream Splitting Method for Magnetohydrodynamics Equations. AIAA JOURNAL, Vol. 47, No. 4

[23]Tan, J. W. Computational Magnetohydrodynamics.

[24] Komitor, A. W. (2023). Comparing Finite Volume and Discontinuous Galerkin Methods for Magnetohydrodynamic Flows (Doctoral dissertation, University of Colorado at Boulder).

[25]Flint, C., & Vahala, G. (2018). A partial entropic lattice Boltzmann MHD simulation of the Orszag–Tang vortex. Radiation Effects and Defects in Solids, 173(1-2), 55-65.

[26] Dahlburg, R. B., & Picone, J. M. (1989). Evolution of the Orszag–Tang vortex system in a compressible medium. I. Initial average subsonic flow. Physics of Fluids B: Plasma Physics, 1(11), 2153-2171.

[27]Dudson, B. D., Umansky, M. V., Xu, X. Q., Snyder, P. B., & Wilson, H. R. (2009). BOUT++: A framework for parallel plasma fluid simulations. Computer Physics Communications, 180(9), 1467-1480.

[28]Huazheng, F., & Xueshang, F. (2014). Splitting based scheme for three-dimensional MHD with dual time stepping. 空间科学学报, 35(1), 9-17.

[29]Feng, X., Liu, X., Xiang, C., Li, H., & Wei, F. (2019). A new MHD model with a rotated-hybrid scheme and solenoidality-preserving approach. The Astrophysical Journal, 871(2), 226.

[30] Feng, X., & Fu, H. (2014, September). Dual Time Stepping Method For three-dimensional MHD With Splitting Based Scheme. In 8th International Conference of Numerical Modeling of Space Plasma Flows (ASTRONUM 2013) (Vol. 488, p. 223).

[31]Jiang, G. S., & Wu, C. C. (1999). A high-order WENO finite difference scheme for the equations of ideal magnetohydrodynamics. Journal of Computational Physics, 150(2), 561-594.

[32]Armstrong, C. K., & Craig, I. J. (2013). Visco–resistive dissipation in

transient reconnection driven by the Orszag–Tang vortex. Solar Physics, 283, 463-471.

[33]Snow, B., Hillier, A., Murtas, G., Botha, G. J., & Camera, S. (2021). Shock identification and classification in 2D magnetohydrodynamic compressible turbulence—Orszag–Tang vortex. Experimental Results, 2, e35.

[34]Tu, X., Wang, Q., Zheng, H., & Gao, L. (2022). Meshless methods for magnetohydrodynamics with vector potential. Journal of Computational Physics, 470, 111596.

[35]Cartes, C., Bustamante, M. D., Pouquet, A., & Brachet, M. E. (2008). Capturing reconnection phenomena using generalized Eulerian–Lagrangian description in Navier–Stokes and resistive MHD. Fluid dynamics research, 41(1), 011404.

[36] Jadhav, K., & Chandy, A. J. (2021). Analysis of energy transfer through direct numerical simulations of magnetohydrodynamic Orszag–Tang vortex. Physics of Fluids, 33(6), 065112.

[37]Nadeem, S., Akhtar, S., Saleem, A., Akkurt, N., Ghazwani, H. A., & Eldin,

S. M. (2023). Numerical computations of blood flow through stenosed arteries via CFD tool OpenFOAM. Alexandria EngineeringJournal, 69, 613- 637.

[38]Cao, Y., Tao, T., Shi, Y., Cao, S., Zhou, D., & Chen, W. L. (2023). Large- eddy simulation of separated turbulent flows over a three-dimensional hill using WRF and OpenFOAM. Journal of Wind Engineering and Industrial Aerodynamics, 236, 105357.

[39]Magacho da Silva, B., Tavares, H. S., Moriconi, L., & Loureiro, J. (2023). DoubleMultiple-Relaxation-Time model of Lattice-Boltzmann Magnetohydrodynamics at Low Magnetic Reynolds Numbers. Physics of Fluids.

[40] Pietersen, F. (2022). Verification of resistivemhdFoam as an MHD Solverfor the 3D Orszag-Tang Vortex and Hartmann Duct Flow (Doctoral dissertation).

[41] Balasubramanian, R., & Anandhanarayanan, K. (2018). Development of an Ideal Magnetohydrodynamics Flow solver for High-Speed Flow Control. Journal of The Institution of Engineers (India): Series C, 99, 489-502.

[42] Yalim, M. S., Abeele, D. V., Lani, A., Quintino, T., & Deconinck, H. (2011). A finite volume implicit time integration method for solving the equations of ideal magnetohydrodynamics for the hyperbolic divergence

cleaning approach. Journal of Computational Physics, 230(15), 6136- 6154.

[43]Tóth, G. (2000). The$\nabla \cdot B = 0$ constraint in shock-capturing magnetohydrodynamics codes. Journal of Computational Physics, 161(2), 605-652.

[44]Tao, Wang, et al. "Comparative study of three AUSM algorithms and simulated application on the solar wind." 空间科学学报 35.4 (2015): 393- 402

[45]C. J. Greenshields. Open foam user guide. Open FOAM Foundation Ltd, version, 3(1),2015

[46] E. Leblebici, “Unsteady atmospheric flow solutions with open foam coupled. with the numerical weather prediction software, WRF,” Ph.D. - Doctoral Program, Middle East Technical University, 2018.

[47] Yusuf, S. N. A., Asako, Y., Che Sidik, N. A., Mohamed, S. B.., & Aziz Japar, W. M. A. (2020). A Short Review of RANS Turbulence Models. CFD Letters, 12(11), 83–96. https://doi.org/10.37934/cfdl.12.11.8396

[48] (n.d.). Turbulent flows. Slide Serve. https://www.slideserve.com/lapis/cfd-modeling-of-turbulent-flows

[49]Garrido González, David. (2020). Non-linear MHD simulations of magnetically confined plasma using OpenFOAM. 10.13140/RG.2.2.14342.40008.

APPENDICES

A. mhdFOAM Codes for B-PISO Loop

```
    fvVectorMatrix UEqn
    (
        fvm::ddt(U)
      + fvm::div(phi, U)
      - fvc::div(phiB, 2.0*DBU*B)
      - fvm::laplacian(nu, U)
      + fvc::grad(DBU*magSqr(B))
    );

    if (piso.momentumPredictor())
    {
        solve(UEqn == -fvc::grad(p));
    }
```

```
while (bpiso.correct())
    fvVectorMatrix BEqn
                (
                    fvm::ddt(B)
                  + fvm::div(phi, B)
                  - fvc::div(phiB, U)
                  - fvm::laplacian(DB, B)
                );

                BEqn.solve();
                ...
```

B. Codestream for B_0

```
#codeStream
{

    codeInclude
    #{
        #include "fvCFD.H"
    #};
    codeOptions
    #{
        -I$(LIB_SRC)/finiteVolume/lnInclude \
        -I$(LIB_SRC)/meshTools/lnInclude
    #};
    codeLibs
    #{
        -lmeshTools \
        -lfiniteVolume
    #};

    code
    #{
        const IOdictionary& d = static_cast<const IOdictionary&>(dict);
            const fvMesh& mesh = refCast<const fvMesh>(d.db());
            vectorField B_0(mesh.nCells(), Foam::Vector<double>(0.,0.,0.));

            forAll(B_0, i)
            {
                const scalar x = mesh.C()[i][0];
                const scalar y = mesh.C()[i][1];
                const scalar z = mesh.C()[i][2];
                B_0[i] = 0.8*Foam::Vector<double>(-2*Foam::sin(2*y)+Foam::sin(z), 2*Foam::sin(2*x)+Foam::sin(z), Foam::sin(x)+Foam::sin(y));
            }

            B_0.writeEntry("",os)   ;
```

C. Codestream for U_0

```
#codeStream
{
    codeInclude
    #{
        #include "fvCFD.H"
    #};
    codeOptions
    #{
        -I$(LIB_SRC)/finiteVolume/lnInclude \
        -I$(LIB_SRC)/meshTools/lnInclude
    #};
    codeLibs
    #{
        -lmeshTools \
        -lfiniteVolume
    #};

    code
    #{
        const IOdictionary& d = static_cast<const IOdictionary&>(dict);
            const fvMesh& mesh = refCast<const fvMesh>(d.db());
            vectorField U_0(mesh.nCells(), Foam::Vector<double>(0.,0.,0.));

            forAll(U_0, i)
            {
                const scalar x = mesh.C()[i][0];
                const scalar y = mesh.C()[i][1];
                const scalar z = mesh.C()[i][2];
                U_0[i] = Foam::Vector<double>(-2*Foam::sin(y), 2*Foam::sin(x), 0.);
            }

            U_0.writeEntry("",os)   ;
    #};
```